Article:
Fang, P, Yan, M, Chi, C et al. (7 more authors) (2019) Brassinosteroids Act as a Positive Regulator of Photoprotection in Response to Chilling Stress. Plant Physiology, 180 (4). pp. 2061-2076. ISSN 0032-0889

https://doi.org/10.1104/pp.19.00088

Running title： BR regulation of photoprotection

Corresponding author details

Jingquan Yu

Department of Horticulture, Zijingang Campus, Zhejiang University, Yuhangtang Road 866, Hangzhou 310058, PR China

Telephone: 0086-571-88982381

E-mail:jqyu@zju.edu.cn

Article title

Brassinosteroids act as a positive regulator of photoprotection in response to chilling stress

Authors: Pingping Fang[1], Cheng Chi[1], ,Mengqi Wang[1], Yanhong Zhou[1,2], Jie Zhou[1], Kai Shi[1], Xiaojian Xia[1], Christine H. Foyer[3] and Jingquan Yu[1, 2*]

[1]Department of Horticulture, Zijingang Campus, Zhejiang University, 866 Yuhangtang Road, Hangzhou, 310058, P.R. China

[2]Zhejiang Provincial Key Laboratory of Horticultural Plant Integrative Biology, 866 Yuhangtang Road, Hangzhou, 310058, P.R. China[3]Centre for Plant Sciences, Faculty of Biology, University of Leeds, Leeds, LS2 9JT, UK

One-sentence summary

Brassinosteroids positive regulate photoprotection via redox-PGR5-mediated pathway in response to chilling stress in tomato

List of author contributions

C.F. and J.Y. designed the research and wrote the manuscript. P.F. performed the experiments and analyzed data. C.C. and M.W. participated in the chilling stress treatment. Y.Z. and X.X. participated in the determination of Chl fluorescence. J.Z. and K.S. participated in organizing and discussion about the writing of the manuscript.

Funding information

This work was supported by the State Key Program of National Natural Science Foundation of China (31430076).

Corresponding author email

jqyu@zju.edu.cn (Jingquan Yu)

ABSTRACT

Photoprotection is an important strategy adopted by plants to avoid photoinhibition under stress conditions. However, the way in which photoprotection is regulated is not fully understood. Here, we demonstrated that mutants of brassinosteroid (BR) biosynthesis (dwf) and its signaling component (bzr1) were more sensitive to photoinhibition at PSII and PSI with decreased cyclic electron flow (CEF) around PSI and non-photochemical quenching (NPQ), accumulation of PSII subunit S (PsbS), violaxanthin de-epoxidase (VDE) and D1. Chilling induced accumulations of brassinolide, 26-castasterone and 28-norcastasterone and activated the signaling component, BZR1, which directly activates the transcription of RESPIRATORY BURST OXIDASE HOMOLOG 1 (RBOH1) with the production of H_2O_2 in the apoplast. While apoplastic H_2O_2 is essential for the induction of PROTON GRADIENT REGULATION5 (PGR5)-dependent CEF, PGR5 participates in the regulation of chilling- and BR-inducted of NPQ, accumulation of D1, VDE and PsbS and activity of several antioxidant enzymes. Mutations in BZR1and PGR5 or suppressed transcription of RBOH1 all compromised chilling- and BR-induced photoprotection with increased sensitivity to photoinhibition. These results strongly suggest that BRs act as a positive regulator of photoprotection in a redox-PGR5-dependent manner in response to chilling stress in tomato.

KEYWORDS: apoplast; brassinosteroids (BRs); BRASSINAZOLE-RESISTANT 1; cyclic electron flow (CEF); chilling stress; reactive oxygen species (ROS); photoinhibition, photoprotection; PROTON GRADIENT REGULATION5 (PGR5); Solanum lycopersicum

INTRODUCTION

In photosynthesis, plants absorb sunlight to power the photochemical reaction. However, excess light absorption can cause an overproduction of reactive oxygen species (ROS), which further induces photodamage in the photosynthetic machinery,

primarily photosystem II (PSII) and photosystem I (PSI), resulting in photoinhibition and decreases in photosynthetic activity, growth and productivity (Triantaphylides and Havaux, 2009; Takahashi and Badger 2011). The degree of photoinhibition is indicated by the decreases in the maximal photochemical efficiency of PSII (Fv/Fm) and in the maximal P700 oxidation (ΔP700max) in PSI. Such events can be exacerbated by stress conditions, such as drought, high or low temperatures, and salinity (Takahashi and Murata, 2008). To avoid the over-reduction of the photosystems that leads to photoinhibition, plants have developed diverse photoprotective strategies, such as the movement of leaves and chloroplasts for light avoidance, ROS scavenging systems, the dissipation of absorbed light energy as heat, cyclic electron flow (CEF) around PSI, the photorespiratory pathway and the repair of damaged PSII (primarily the D1 protein) (Murchie and Niyogi, 2011; Takahashi and Badger 2011; Goss and Lepetit, 2015).

Higher plants have several enzymatic and non-enzymatic processes to scavenge ROS and prevent oxidative damage. In chloroplasts, the Foyer-Halliwell-Asada cycle, consisting of superoxide dismutase (SOD), ascorbate peroxidase (APX), monodehydroascorbate reductase (MDAR), dehydroascorbate reductase (DHAR), and glutathione reductase (GR), and non-enzymatic antioxidants such as carotenoids, contributes greatly to the scavenging of ROS that accumulated in the chloroplasts (Asada, 2006; Takahashi and Badger, 2011). Deficiencies in Foyer-Halliwell-Asada cycle enzymes increased photoinhibition while overexpression of the genes encoding these enzymes tended to decrease photoinhibition (Foyer et al., 1995; Maruta et al., 2010).

The photoprotective thermal dissipation of excessive excitation energy is measured as the non-photochemical quenching of chlorophyll fluorescence (NPQ) (Jahns and Holzwarth, 2012). In this mechanism, the electron transport in the chloroplasts generate a pH gradient across thylakoid membranes (ΔpH), and the ΔpH-dependent NPQ known as energy-dependent quenching (qE) is associated with the conversion of violaxanthin to zeaxanthin via violaxanthin de-epoxidase (VDE) and the protonation of the PSII subunit S (PsbS) in plants (Goss and Lepetit, 2015). The importance of PsbS, VDE and NPQ in protecting the photosynthetic machinery has

been identified previously in the plant kingdom (Li et al., 2000; Pinnola et al., 2013; Ikeuchi et al., 2014). However, their precise regulation mechanism remains unclear.

The CEF, which leads to the generation of a ΔpH across thylakoid membranes, driving ATP synthesis without producing NADPH, is important for the activation of qE (Johnson, 2011). In Arabidopsis, the CEF around PSI consists of two routes (Munekage et al., 2004), namely (i) the antimycin A-sensitive pathway, which depends on PROTON GRADIENT REGULATION 5 (PGR5) and PGR5-LIKE PROTEIN1 (PGRL1) and (ii) the antimycin A-insensitive pathway, which is mediated by the chloroplast NADH dehydrogenase-like (NDH) complex. The qE was severely impaired in the pgr5 mutant but not affected in the plants that lack chloroplast NDH, suggesting that PGR5/PGRL1-dependent PSI cyclic electron transport contributes markedly to the formation of the ΔpH (Nishikawa et al., 2012; Hashimoto et al., 2003). The loss of function of proteins involved in CEF around PSI increased the sensitivity of plants to photoinhibition at PSII and PSI (Munekage et al., 2002). Additionally, plants have evolved the ability to prevent photoinhibition by integrating these photoprotective pathways. For example, a lack of CEF component PGR5 resulted in decreased qE with an increased extent of photoinhibition while an increased accumulation of ROS led to the inhibition of D1 protein synthesis (Steinbeck et al., 2015; Takahashi et al, 2009). However, the ways in which these processes are coordinated remains ambiguous, especially in plants that were exposed to stress conditions.

While excess accumulation of ROS has effects on lipid peroxidation as well as on proteins and nucleic acids oxidation and thus accelerate photoinhibition, ROS produced in the apoplast play beneficial roles in the regulation of growth, development and defense (Garg and Manchanda, 2009). ROS produced by NADPH oxidase are known to act as important signaling components and function in signaling pathways (Zurbriggen et al., 2010; Xia et al., 2009, 2017). Concomitantly, ROS have been observed to activate CEF in vitro and in vivo (Lascano et al., 2003; Strand et al., 2015). Consistent with these findings, ROS such as H_2O_2 participate in the regulation of NDH complex expression or the accumulation of NDH proteins (Casano et al., 2001; Strand et al., 2015). These results indicate that ROS could be involved in regulating

photosynthesis and photoprotection. However, it is still unclear how these ROS are regulated and whether they participate in other photoprotection processes.

Brassinosteroids (BRs) are the class of steroid plant hormones that play important roles in plant growth, development and stress responses. BRs are perceived by a leucine-rich repeat receptor-like kinase BRASSINOSTEROID INSENSITIVE1 (BRI1). BRI1 interacts with BRI1-ASSOCIATED RECEPTOR KINASE 1 (BAK1), and positively regulates BRASSINAZOLE-RESISTANT 1 (BZR1) and BRI1-EMSSUPPRESSOR1 (BES1) which are essential positive regulators of BR signaling (Clouse, 2011). An increase in BR level leads to BZR1 dephosphorylation, promoting the binding of dephosphorylated BZR1 (dBZR1) to the conserved E –box (CANNTG) and/or to the BRRE element (CGTGT/CG) in the promoters of BR-responsive target genes (He et al., 2005; Sun et al., 2010; Li et al.,2017). A large number of studies have shown that BR enhances stress tolerance and ameliorates cellular damages caused bytemperature , salinity, drought and heavy metal stresses (Bajguz & Hayat, 2009; Xia et al., 2009). Previously, we found that BRs could enhance photosynthesis, stress tolerance and the activity of antioxidant enzymes in an apoplastic H_2O_2-dependent manner (Zhou et al., 2014; Xia et al., 2017). In addition, overexpression of the BR biosynthesis-limiting gene DWARF resulted in an increased biosynthesis of carotenoids in tomato plants (Li et al., 2016).Given the role of apoplastic H_2O_2 in regulating CEF and carotenoids during photoprotection by scavenging ROS and dissipating excess energy into heat, it is highly plausible that BR could positively regulate the photoprotection process, resulting in a decreased degree of photoinhibition. Here, we found that BR plays a critical role in regulating photoprotection in response to chilling stress. Induction by cold and BR, BZR1 directly activates the transcript of RBOH1 and the generation of apoplastic H_2O_2, subsequently induced the PGR5-dependent CEF, NPQ, and accumulation or activity of proteins involved in photoprotection.

RESULTS

BR levels, photoinhibition and photoprotection

We first determined whether the BR levels are linked to photoprotection in response to chilling by comparing the degree of photoinhibition at PSII and PSI for plants with the same genetic background that differ in their BR biosynthesis capacity, i.e., dwf, the mutant with a lesion in the BR biosynthetic gene DWARF (encoding CYP85A1; ZZZZ); the wild type (WT), and DWF:OE, transgenic plants overexpressing DWARF (Li et al., 2016). Under control conditions, no significant differences were observed in the maximum quantum efficiency of photosystem II (Fv/Fm), maximum P700 photooxidation level ($\Delta P700_{max}$) and relative electrolyte leakage (REL) among the three genotypes used here. After being exposed to a chilling condition at 4°C for 6 d, all these plants showed decreases in Fv/Fm and $\Delta P700_{max}$ and increases in REL (Fig. 1A; Supplemental Fig. S1). However, the dwf plants had significantly lower while the DWF:OE plants had higher Fv/Fm and $\Delta P700_{max}$ values relative to the WT plants. Consistent with this finding, the dwf plants had significantly higher RELs while the DWF:OE plants had lower RELs relative to the WT plants after being exposed to chilling stress (Supplemental Fig. S1). The chilling stress induced an increase in the value of non-photochemical quenching of chlorophyll fluorescence (NPQ), energy-dependent quenching (qE), as well as the cyclic electron flow (CEF) (Fig.1, B and C; Supplemental Fig. S2). In comparison to the WT plants, there were less increases in the NPQ, qE and CEF in the dwf plants and greater increases in the NPQ, qE and CEF in DWF:OE plants. A qRT-PCR analysis revealed that chilling stress induced the accumulation of PGR5 transcripts with the level in DWF:OE plants being the most abundant (Fig. 1D). However, chilling stress differentially suppressed the expression of PGRLA1 and PGRLA2, and ORR, which encodes the NDH complex subunit (Supplemental Fig. S3).Under control conditions, the accumulation of PSII subunit S (Psbs), violaxanthin de-epoxidase (VDE) and D1 proteinsincreased with the increase in BR levels in the plants (Fig. 1E). The accumulation of of PsbS and VDE proteins increased whilst that D1 protein decreased after a chilling stress in all of these plants. However, dwf plants had lower whilst DWF:OE plants had higher accumulation of these proteins after the stress.

Chilling induced BR biosynthesis and BZR1 accumulation

To determine whether plants respond to cold by increasing BR biosynthesis, we analyzed the changes in the endogenous BRs in the leaves exposed to 25℃ and 4℃ for different durations. UHPLC-ESI–MS/MS analysis revealed that the content of brassinolide (BL), 26-castasterone (CS) and 28-norcastasterone (28-norCS) in the leaves were stable under the control conditions but were up-regulated by chilling treatment. Within the first 6 h, chilling treatment led to a significant increase in BR contents as BL，CS and 28-norCS increased by 1.7-, 1.8- and 1.97- fold respectively (Fig. 2A). However, the content of BRs declined gradually and was different from those at 25℃ at 24 h. To figure out whether DWARF transcript affects the accumulation of BRs under chilling stress. Leaves were collected from dwf, WT and DWF:OE at 6 h after chilling for the determination of BRs. Under control condition, DWARF overexpression increased the accumulation of BL, CS and 28-norCS by 9%, 28.7% and 291%, respectively. Conversely, mutation of DWARF (dwf) decreased CS and 28-norCS by 71.9% and 78.6%. After being exposed to 4℃ for 6 h，all plants showed increased accumulations of BRs. However, the dwf plants had significantly lower while the DWF:OE plants had higher contents of BL，CS and 28-norCS relative to the WT plants (Fig. 2B). These results indicated plants respond to chilling stress by increasing BR biosynthesis.

We next examined how BR signaling was altered by the chilling stress and exogenous BR. Western bolt showed that the accumulation of dephosphorylated BZR1 (dBZR1) was increased after application of 24-epibrassinolide (EBR, 0.2μM) at 25°C (Fig. 2C). Exposure to chilling at 4℃ increased the accumulation of both phosphorylated BZR1 (pBZR1) and dBZR1, especially in the presence of EBR. Notably, the ratio of dBZR1 to pBZR1 was increased by both EBR application and chilling treatment. It from from 0.05 for plants at 25℃ to 0.17 in the plants after a chilling for 12 h with EBR pretreatment (Fig. 2C). Therefore, both the BR and chilling activated BR signaling.

BZR1, photoinhibition and photoprotection

We then determined whether BZR1, a transcriptional factor involved in BR signaling, participates in BR regulation of photoinhibition. We found bzr1 mutants had increased sensitivities to chilling-induced photoinhibition as indicated by the lower Fv/Fm and $\Delta P700_{max}$ in bzr1 plants relative to the WT plants (Fig. 3A). Consistently, the bzr1 plants had significantly higher RELs relative to the WT plants after being exposed to chilling stress for 6 d (Supplemental Fig. S4). Importantly, application of EBR increased Fv/Fm,$\Delta P700_{max}$ and decreased REL in WT plant but not in bzr1 mutants. While there were little differences in the NPQ, qE, transcript of PGR5 and CEF between the WT and bzr1plants, foliar applications of EBR increased the NPQ, transcript of PGR5 and CEF in the WT plants but not in the bzr1 plants at 25°C (Fig. 3, B-D; Supplemental Fig.S5). Importantly, chilling stress induced an increase in NPQ, qE, transcript of PGR5 and CEF to a lesser degree in bzr1 plants as compared with the WT plants (Fig. 3, B-D Supplemental Fig.S5). Similarly, the bzr1 plants showed a compromised response to EBR application at 4 °C. Western blot analysis revealed that mutation in BZR1 resulted in a decreased accumulation of D1, PsbS and VDE proteins and compromised EBR-induced accumulation of these photoprotection related proteins in response to chilling stress (Fig. 3E).

Transcriptional activation of RBOH1 by BZR1

Previously, we reported that BR induced a RESPIRATORY BURST OXIDASE HOMOLOG 1 (RBOH1)-dependent production of H_2O_2 in the apoplast of tomato and cucumber plants (Xia et al., 2009, 2017). Here we found chilling- and EBR application-induced expression of RBOH1 and accumulation of H_2O_2 both in the apoplast and leaf tissues in WT plants but not in bzr1 plants (Fig. 4A and B; Supplemental Fig.S6). Given that there are several BRRE and E-box motifs in the promoter sequence of RBOH1 (Fig. 4C), we explored the possibility of BZR1 binding to the RBOH1 promoter. Firstly, in vitro detection was performed using yeast one-hybrid (Y1H) analysis. In which a 1937-bp promoter sequence of RBOH1 was cloned into the pAbAi vector to construct pAbAi-bait. As shown in Fig. 4D, yeast cells containing the bait vector harboring RBOH1

promoter segments grew on the selection medium with 100 ng/ml Aureobasidin A (AbA) when transformed with BZR1-AD, while that transformation with empty pGADT7 vector failed to grow on the same medium. To further confirm the binding results, we performed in vivo analysis by ChIP-qPCR. Considering that the BZR1 protein from tomato leaves existed mainly in pBZR1 status under control conditions, we thus treated the 35Spro:BZR1-HA plants with chilling to induce the accumulation of dBZR (Fig 2. C)1.Results shown that the RBOH1 promoter fragment was enriched 5.7 fold in fractions immunoprecipitated with the anti-HA antibody in the 35Spro:BZR1-HA line compared with WT plants. However, the IgG control antibody failed to pull down these DNA segments (Fig. 4E). Y1H assay, together with ChIP-qPCR, confirmed that BZR1can directly bind to the promoter of RBOH1 in vitro and in vivo. These results demonstrate that BZR1 induces the production of apoplastic H_2O_2 through a directly regulation on RBOH1 at transcriptional level.

Role of apoplastic H_2O_2 in regulating photoprotection

To determine whether the BR-dependent production of H_2O_2 in the apoplast plays a role in regulating photoprotection, we compared the Fv/Fm and $\Delta P700_{max}$ in the WT and RBOH1-RNAi plants after exposing them to the chilling stress at 4°C for 6 d. Although no significant differences were found in the Fv/Fm,$\Delta P700_{max}$ and REL between WT and RBOH1-RNAi plants grown at 25°C, chilling stress induced more significant decreases in Fv/Fm and $\Delta P700_{max}$ and increases in REL in the RBOH1-RNAi plants compared to the WT plants (Fig. 5A; Supplemental Fig. S7). Although foliar application of EBR increased the Fv/Fm and $\Delta P700_{max}$ and decreased the REL in WT plants, it had few effects on these parameters in the RBOH1-RNAi plants. While there were no significant differences in the NPQ values between the WT and RBOH1-RNAi plants at 25°C, foliar applications of EBR increased the NPQ in the WT plants but not in the RBOH1-RNAi plants (Supplemental Fig. S8A). Importantly, chilling stress induced increases in NPQ and qE to a lesser degree in RBOH1-RNAi plants compared with the WT plants (Fig. 5B, Supplemental Fig. S8B). Again, the RBOH1-RNAi plants showed a compromised response to EBR application at 4 °C.

To determine whether BR-induced CEF is RBOH1-dependent, we compared the CEF in the WT and RBOH1-RNAi plants with chilling and/or EBR treatment. We found that the CEF in the RBOH1-RNAi plants was not significantly different from that in

WT plants at 25°C. Chilling stimuli induced the CEF in WT plants, such an induction was, however, less significant in the RBOH1-RNAi plants. (Fig. 5C). Remarkably, EBR application only induced the CEF in WT plants, but not in the RBOH1-RNAi plants regardless of the growth temperatures (Fig. 5C). Consistent with the changes in the CEF, chilling-induced expression of PGR5 was partially abolished in RBOH1-RNAi plants. Similarly, the EBR application induced the expression of PGR5 only in WT plants but not in RBOH1-RNAi plants regardless of the growth temperatures (Fig. 5D). Western blot analysis revealed that silencing of RBOH1 inhibited the accumulation of PsbS and VDE proteins induced by EBR application in response to chilling stress (Fig. 5E). Chilling suppressed the accumulation of D1 protein in both WT plants and RBOH1-RNAi plants, while EBR application alleviated the loss of D1 in the WT plants but not in the RBOH1-RNAi plants (Fig. 5E).

Role of CEF in BR-induced photoprotection

To determine whether PGR5 mediated BR-induced photoprotection in response to chilling, we used a pgr5 mutant generated using a CRISPR/cas9 technique (Wang et al., 2018). The growth of the pgr5 mutant did not differ from that of the WT plants at 25°C . In addition, there was little difference in the Fv/Fm and the $\Delta P700_{max}$ between the WT and pgr5 mutant (Fig. 6A). However, a chilling treatment at 4°C induced more significant decreases in the Fv/Fm and $\Delta P700_{max}$ and an increase in REL in the pgr5 mutant compared with the WT plants (Fig. 6A; Supplemental Fig. S9B). Although the EBR application increased the Fv/Fm and $\Delta P700_{max}$ and decreased the REL in WT plants after chilling, this beneficial effect was not observed in the pgr5 mutant.

We then analyzed the changes in NPQ and qE in WT plants and pgr5 mutant with or without the chilling treatment. When the pgr5 mutant was grown at 25°C, the plants showed lower NPQ and qE values relative to the WT plants, and there was an EBR-induced increase in the NPQ and qE in the WT plants (Supplemental Fig. S10; Fig. 6B). Significantly, chilling induced the NPQ and qE in the WT plants but not in the pgr5 mutant. EBR application significantly increased the NPQ and qE in the WT plants with the effects being more significant in plants at 4°C, but it had negligible effects on the NPQ and qE in pgr5 mutant regardless of the growth temperature (Fig. 6B; Supplemental Fig. S10). Consistent with the role of PGR5 in the CEF, pgr5 mutant showed much less CEF, and the CEF was almost not responsive to foliar EBR applications (Fig. 6C). Chilling induced the CEF in WT plants, which was particularly

significant after EBR treatment. However, both chilling and EBR failed to increase the CEF in the pgr5 mutant (Fig. 6C). Furthermore, pgr5 mutant had decreased accumulation of PsbS, VDE and D1 proteins relative to WT plants and this was especially apparent at 4°C. Significantly, foliar EBR applications failed to increase the accumulation of PsbS, VDE and D1 proteins (Fig. 6D).

We also examined the response of the antioxidant enzyme activities to the chilling and EBR in WT plants and pgr5 mutant. At a growth temperature of 25°C, there were no significant differences in the activity of APX, GR and MDAR between the WT plants and pgr5 mutant. However, the pgr5 mutant had decreased DHAR activity compared to the WT plants. The application of EBR resulted in an increased activity of these antioxidant enzymes in WT plants but not in pgr5 mutant. Although the chilling significantly induced the activities of antioxidant enzymes including APX, GR, MDAR and DHAR in the WT plants, it had little effect on the activity of these enzymes in pgr5 mutant with the exception of DHAR, which was induced by 30%. Again, the foliar application of EBR only induced the activity of these antioxidant enzymes in the WT plants, and the PGR5 mutation compromised the EBR-induced activation of these antioxidant enzymes (Fig. 7).

DISCUSSION

The induction of different photoprotection pathways is critical for plants to avoid photoinhibition (Murchie and Niyogi, 2011). However, the regulators of these photoprotective pathways are largely unknown.

Here, data are presented to show that BR signaling plays a critical role in the alleviation of photoinhibition at both PSII and PSI by activating photoprotection. Cold induces increases in BR biosynthesis and the accumulation of dBZR1. BZR1 directly activates the transcript of RBOH1 with the production of apoplastic H_2O_2, leading to improved photoprotection by enhancing NPQ through increasing CEF and VDE. PGR5-dependent CEF is important for the induction of NPQ, as well as VDE and PsbS. In addition, PGR5 also plays a role in the induction of antioxidant response and D1 in PSII repair (Fig. 8).

BR signaling is involved in regulating photoprotection

Earlier studies demonstrated that BR participates in the regulation of chlorophyll biosynthesis, the accumulation of photosynthetic proteins and PSII efficiency and in the activation of Benson-Calvin cycle enzymes in higher plants (Oh et al., 2011; Ogweno et al., 2008; Xia et al., 2009, 2017). Here, we found that sensitivity to photoinhibition is related to the BR levels and BR signaling element BZR1in tomato plants. Compared to the WT plants, mutants of the BR-deficient dwf and BR signaling-deficient bzr1 had lower while plants overexpressing DWARF had higher Fv/Fm and $\Delta P700_{max}$ values after exposure to chilling stress (Figs. 1A and 3A). Consistent with DWARF overexpression, foliar applications of EBR also alleviated chilling-induced photoinhibition (Figs. 3A, 5A and 6A). These results suggested that BR signaling is important for the photoprotection at both PSII and PSI. Given the predominant occurrence of chilling stress for thermophilic plants in winter-spring period, the manipulation of BR biosynthesis-related or signaling genes or the exogenous application of synthetic BR could be potential approaches for alleviating photoinhibition in these plants.

Although exogenous BR has been found to alleviate stress-induced photoinhibition in our previous studies, no in-depth study has been performed to examine the underlying mechanism (Ogweno et al., 2008, Xia et al., 2017). Data from the present study supported the idea that BR-induced photoprotection partially contributed to the alleviation of photoinhibition. There was a more intense increase in NPQ, qE and CEF in DWF: OE plants after a chilling treatment, whereas NPQ, qE and CEF in BR biosynthesis mutant dwf and BR signaling-defective mutants bzr1were lower relative to the WT plants (Figs. 1, B and C; 3, B and C; Supplemental Figs. S2 and S5). Similarly, EBR application increased the NPQ, qE and CEF in WT plants (Figs. 3, B and C; Supplemental Figs. S5). Apparently, BR biosynthesis and signaling are linked to the regulation of NPQ, qE and CEF in response to chilling. It is well known that PsbS-mediated conformational changes in the light-harvesting chlorophyll-protein complex II (LHCII) participate in ΔpH-dependent energy quenching (Li et al., 2000, Murchie and Niyogi., 2011). In the xanthophyll cycle, VDE catalyzes the conversion from violaxanthin (V) into zeaxanthin (Z) in response to light, whereas Z regulates the

dissipation of the excess absorbed energy as heat (Niyogi et al., 1998; Goss and Lepetit, 2015). The de-epoxidation state of the xanthophyll cycle pigments is thought to regulate qE-dependent NPQ (Kromdijk et al., 2016). Defect in VDE activity increases the extent of PSII photoinhibition (Niyogi et al., 1998; Han et al., 2010). Here, we found that BR biosynthesis and signaling positively regulate the accumulation of PsbS and VDE proteins in response to changes in the growth environment (Figs. 1E and 3E). Meanwhile, D1 repair is thought to contribute to the chilling tolerance in some species, and our data support the idea that a high level of BR maintained the high D1 protein content before and after chilling stress and BR-induced photoprotection may involve a D1 repair process (Figs. 1E and 3E).

Plants usually accumulate anti-stress hormones like abscisic acid (ABA), salicylic acid (SA) and jasmonates (JAs) in response to stress stimuli. For example, cold, drought and heat stresses induce an increase in ABA accumulation whilst plants usually accumulate SA or JAs in response to pathogens or herbivores attack (Small & Degenhardt et al., 2018; Lv et al., 2018). Here, we firstly found that chilling stress induced the accumulations of active BRs in the leaves (Fig. 2A). Further more, overexpression of DWARF transcript not only up-regulated BR contents under control condition but also induced higher accumulations of BRs under chilling stress (Fig. 2B). Therefore, the activated photoprotection processes under chilling conditions were related to the increased BR biosynthesis. It is well known that the execution of BR responses needs the activation of BR signaling elements. BZR1, the important one of them, was found to be induced by chilling stress and BR application. The ratio of dephosphorylated BZR1 to phosphorylated BZR1, a readout of BR signaling, was also increased by both chilling and BR treatment. (Fig. 2C). Therefore, while the basal level of BRs is important for the cold response, the activation of BZR1 by the increased biosynthesis BR is critical for the cold response (Figs.1-3).

BZR1-activated RBOH1 is critical for BR-induced photoprotection

Accumulations of ROS, such as the superoxide radicals and singlet oxygen increase when more electrons are released from the chloroplast electron transport chain than the electron-consuming capacity of the Benson-Calvin cycle under stress conditions

(Allakhverdiev and Murata, 2004； Allakhverdiev et al., 2007; Takahashi and Murata,2005,2008). The over-accumulation of ROS in the chloroplast inhibits the translation of PsbA mRNA (which encodes D1 protein), thus inactivating the PSII repair process with photoinhibition (Nishiyama et al., 2006; Takahashi and Murata, 2008). However, recent studies showed that ROS generated in the apoplast may function as a signal in cold response (Xia et al., 2009; Zhou et al., 2014). Here we found that RBOH1-RNAi plants exhibited increased degree of photoinhibition at both PSII and PSI, as indicated by the lower Fv/Fm and $\Delta P700_{max}$ in RBOH1-RNAi plants relative to those in WT plants in response to the chilling treatment (Fig. 5A). Significantly, the EBR-induced alleviation of photoinhibition at either PSII (Fv/Fm) or PSI ($\Delta P700_{max}$) was impaired in RBOH1-RNAi plants (Fig. 5A). These results suggested that RBOH1 is involved in the regulation of photoinhibition and suggested that ROS in the apoplast play a role different from those in chloroplast. This set of results also allows us to argue that BRs alleviate photoinhibition at either PSII or PSI in an RBOH1-dependent manner.

It has been long observed that RBOHs-dependent ROS production mediates BR-induced stress response, it remains scanty how transcript of RBOHs is activated (Xia et al.,2009, 2015; Deng et al., 2016; Jakubowska & Janicka ; 2017). In our study, transcript of RBOH1, the principle RBOHs in tomato (Zhou et al., 2014), was correlated to BZR1 levels in response to cold and BR stimuli (Fig. 4A). Consistent with the correlation of BZR1 levels and transcript of RBOH1, Y1H and ChIP-qPCR assays demonstrated that BZR1 could directly bind to the promoter of RBOH1, thereby activating the transcript of RBOH1 (Fig. 4). These results provided direct evidences for role of BR in the triggering the production of H_2O_2 in the apoplast by BZR1 binding to the promotor of RBOH1.

Until now, it remains unknown whether RBOH1 is also involved in regulating other photoprotection pathways. Here, we found that RBOH1-RNAi plants showed decreased CEF, qE and NPQ with decreased accumulation of D1, PsbS and VDE in response to a chilling treatment (Fig.5, B, C and E; Supplemental Fig. S8). Apparently, the decreased photoprotection ability in RBOH1-RNAi plants contributed the increased degree of photoinhibition. Significantly, EBR-induced CEF, qE, and NPQ and the accumulation

of PsbS, VDE and D1 were abolished in RBOH1-RNAi plants (Fig. 5, B, C and E; Supplemental Fig. S8). All these results suggested that BR-induced photoprotection is largely mediated by apoplastic H_2O_2.

PGR5-mediated CEF plays a critical role in BR-induced photoprotection

The CEF around PSI, a redox-sensitive process, is involved in photoprotection; however, little is known about the regulation mechanism for CEF (Strand et al., 2015; Guo et al., 2016). CEF involves (NDH) complex-dependent and PGR5/PGRL1 complex-dependent pathways that are required to acidify the thylakoid lumen sufficiently to induce qE (Munekage et al., 2002, 2004; Shikanai and Yamamoto, 2017). Among the four genes (PGR5, PGR5-LikeA1, PGR5-LikeA2 and ORR) involved in CEF, only the transcript of PGR5 was induced by chilling and regulated by BR levels, BR signaling (BZR1) and RBOH1 transcript, whilst mutation in PGR5 compromised BR- and chilling–induced CEF (Figs.1D, 3D and 5D; Supplemental Fig.S3). All these results suggested a regulation role of BR-BZR1-apoplstic H_2O_2 signaling in the induction of PGR5-dependent CEF.

Usually, CEF triggers NPQ by activation of the qE through the generation of a ΔpH across the thylakoid membrane (Shikanai and Yamamoto, 2017). Consistent with this, pgr5 mutant had decreased qE values in response to chilling compared to WT plants (Fig. 6B). Interestingly, we found that chilling induced lower NPQ and qE with less accumulation of D1, PsbS and VDE in pgr5 plants as observed in bzr1 and RBOH1-RNAi plants compared to WT plants (Figs. 3, B and E; 5, B and E; 6, B and D; Supplemental Figs. S5, B and S8，B). Furthermore, EBR applications increased their accumulation in WT plants but not in pgr5 plants (Fig. 6, B and D).These results suggested that BR/chilling-induced, ROS-mediated and PGR5-dependent CEF may induce the qE and NPQ by activating the VDE-dependent xanthophyll cycle and the protonation of the PSII subunit protein PsbS in plants. The synthesis de novo of D1 protein is required for the repair of PSII, and the translation of D1 protein synthesis is regulated by the ATP: ADP ratio and the stromal redox potential (Danon 2002; Takahashi and Badger 2011). Previously, we observed that the activation of CEF is linked to an increased generation of ATP (Guo et al., 2016). Therefore, further works on the regulatory role of CEF in APT production and redox homeostasis in response to stress in photoprotection are highly warranted. It is also worth noting that CEF not only

directly plays a role in photoprotection or indirectly by the induction of light dissipation, CEF is also important for the induction of antioxidant reaction as that antioxidant enzymes involved in the Foyer-Halliwell-Asada cycle showed compromised response in the pgr5 plants in response to chilling and EBR application (Fig. 7). Until now, little is known about the relation of CEF and antioxidant reaction in the chloroplast, it will be of great interest to study how CEF participates in the regulation of antioxidant reactions.

Induction of the PGR5-dependent photoprotection is linked to the alleviation of photoinhibition (Fig. 6A). Consistent with earlier observations showing that the impairment of the PGR5-dependent pathway causes acceleration of photoinhibition at PSII and PSI in Arabidopsis (Munekage et al., 2002; Takahashi et al., 2009), we observed more significant decreases in the Fv/Fm and $\Delta P700_{max}$ in the tomato pgr5 mutant as compared with its wild type after a chilling treatment (Fig. 6A). The increased degree of photoinhibition at PSII and PSI in pgr5 mutant was accompanied with a decreased capacity for thermal dissipation as shown by the decreased qE and NPQ with less accumulation of D1, PsbS and VDE in response to chilling (Fig. 6, B and D). These results provided strong evidences for the role of qE-dependent NPQ in preventing the plants from photoinhibiiton as observed in Arabidopsis (Li et al.,2002;Takahashi et al., 2009).

In conclusion, we demonstrated that BR- and chilling-induced BR signaling plays a critical role in alleviating photoinhibition by induction of H_2O_2-CEF-dependent photoprotection pathway (Fig. 8). Chilling and BR-induced accumulation of dBZR1 triggers the production of apoplastic H_2O_2 by directing activating the transcription of RBOH1. H_2O_2-activated PGR5-dependent CEF is essential for the BR-induced accumulation or activity of several antioxidant enzymes and proteins in photoprotection. Results provided strong evidences for BRs as a positive regulator of photoprotection in a redox-PGR5-dependent manner in response to chilling stress in tomato.

MATERIALS AND METHODS

Plant materials and Growth conditions

Tomato (Solanum lycopersicum L.) cultivars Condine Red (CR) and Ailsa Craig (AC) were used as wild types (WT) in this study. The BR biosynthesis mutant dwf (accession LA0571) was obtained from the Tomato Genetics Resource Center

(University of California, Davis, CA, USA). DWF:OE (DWARF-overexpressing line), 35Spro:BZR1-HA (transgenic line with HA tag), CRISPR/Cas9 transgenic lines of bzr1 and pgr5, RBOH1-RNAi-silenced line selected in our laboratory were used in this study (Li et al., 2016; Wang et al., 2018a,b; Yin et al., 2018).

Seedlings were grown in pots using a mixture of peat and vermiculite (3:1, v/v) and receiving Hoagland nutrient solution. The growth conditions were as follows: white light with a 12-h photoperiod, temperature of 25/20℃(day/night), and photosynthetic photo flux density (PPFD) of 200 μmol m^{-2} s^{-1} . Seedlings of Five-week-old were used for subsequent experiments.

Chilling and BR treatment

All experiments were carried out in environmentally controlled growth chambers (model no. E15; Conviron, Canada) with white light of a 12-h photoperiod, and a PPFD of 200μmol m^{-2} s^{-1}. For chilling stress treatment, the plants of different genotypes were treated at 4°C for six days. To determine the effects of exogenous BR, WT, bzr1, RBOH1-RNAi, or pgr5 mutant plants were pre-treated with 24-epibrassinolide (EBR, 0.2 μM, Sigma, USA) 24 h before the chilling treatment. Leaf samples were collected immediately at the end of the treatment to determine the electrolyte leakage. To analyze the gene expression, the accumulation of PsbS, VDE and D1 proteins and the activity of antioxidant enzymes, leaf samples were collected within 24 h after the chilling stress treatment.

Measurements of chilling tolerance and chlorophyll fluorescence

The relative electrolyte leakage was determined as described previously (Wang et al., 2016). The Fv/Fm and NPQ were measured with an Imaging-PAM Chlorophyll Fluorometer (IMAG-MAXI, Heinz Walz, Effeltrich, Germany). Before measurements, plants were dark-adapted for 30 min. The chlorophyll fluorescence parameters were calculated as follows: Fv/Fm = (Fm-Fo)/Fm (Oxborough and Baker, 1997), NPQ = (Fm- Fm')/Fm' (Baker, 2008). The initial fluorescence (Fo) was determined after switching on the measuring beam, followed by a 0.8 s saturating pulse (>4000 μmol m-2s-1) to obtain maximum fluorescence yield (Fm) in plants in the dark. Fm' is the maximum fluorescence yield under 1200 umol $m^{-2}s^{-1}$ of actinic light and Fs is the steady-state fluorescence yield during actinic illumination. The energy-dependent

quenching (qE), the maximum P700 photooxidation level ($\Delta P700_{max}$) and CEF around PSI were measured with the Dual-PAM-100 system (Heinz Walz, German) as described by Wang et al (2018a). CEF around PSI was detected as a transient increase in Chlorophyll Fluorescence after turning off the actinic light (AL, 250 μmol m^{-2} s^{-1} for 3 min).

Quantification of endogenous BRs

The 4th leaf from each tomato plant at 6-leaf stage was used for the analysis of endogenous brassinosteroids. Samples were prepared and determined according to Luo et al (2018). Briefly, 0.1g FW tomato leaves were ground into powder with liquid nitrogen and 1.0 ml of ice cold ACN was added as extraction solution. Deuterium-labelled brassinosteroids including [26-$^2H_3$]-castasterone (0.1ng, OlChemIm, Olomouc, Czech Republic), [28-$^2H_3$]-norcastasterone (0.1ng, OlChemIm, Olomouc, Czech Republic) and [26-$^2H_3$]brassinolide (0.1ng, OlChemIm, Olomouc, Czech Republic) were spiked into the extraction solution as internal standards. After being extracted overnight at 4°C, samples was centrifuged (10,000g) at 4°C for 10 min. The supernatant was transferred into a 10 ml centrifuge tube which contained 0.3g MCX@BBII and 3ml H_2O and then was vigorously stirred for 5 min. After centrifugation (10,000g) at 4°C for 1 min, the pellets obtained was vigorously stirred in 5ml 90% acetone(9:1,v/v; 0.5%FA was added) for 1min. After centrifugation (10,000g) at 4°C for 1 min, the supernatant was discarded and 1.2ml 90% acetone (9:1, v/v) followed with 20-50mg CH_3COONH_4 was added. After being vigorously stirred for 1min and centrifuged (10,000g, 3 min), the upper phase was evaporated to dryness under mild nitrogen stream. Afterwards, sample residue was re-dissolved in 100 μl 45% ACN and analyzed by using UPLC-MS/MS on an Agilent 1290 infinity HPLC system coupled to an Agilent 6460 Triple Quad LC-MS device.

Quantification, histochemical analysis, and cytochemical detection of H_2O_2

H_2O_2 was extracted from 0.3 g leaf samples and determined with spectrophotometry–colorimetry at 415 nm according to the description in our earlier study (Xia et al., 2009). The cytochemical detection of H_2O_2 was visualized using

cytochemical CeCl3 staining and transmission electron mi-croscopy (H7650; Hitachi) as described previously (Xia et al., 2009).

Western blot analysis

For protein extraction, leaf samples were ground into powder in liquid nitrogen and homogenized in extraction buffer (100 mM HEPES,pH7.5,5 mM EDTA,5 mM EGTA, 10 mM Na3VO4,10 mM NaF,50mM β-glycerophosphate,1 mM phenylmethylsulphonyl fluoride,10% glycerol ,7.5 % polyvinylpolypyrrolidone (PVP) and 0.2% β-mercaptoethanol), followed by centrifugation at 13,000g for 20 min. After adjusting the concentration to the same level, proteins were then mixed with 5× loading buffer (125mM Tris-HCl,pH6.8, 5 %[W/V]SDS,25%[v/v] glycerol, 25%[v/v]β-mercaptoethanol, 3.13 mg bromophenol blue/5mL buffer) and heated at 95°C for 10 min. SDS–polyacrylamide gel [12% (w/v)] electrophoresis (SDS-PAGE) was performed to separate the protein extracts.

For PsbS, VDE and D1 detection, antibodies specific to the PsbS, VDE and D1 proteins (Agrisera, Vännäs, Sweden) were used and followed incubation with goat anti-rabbit HRP-linked antibody (Cell Signaling Technology 7074; Danvers, MA, USA).

For BZR1 detection, A mouse monoclonal antibody recognizing HA(Pierce 26183; Rockford, IL, USA) was used and followed incubation with a goat anti-mouse IgG antibody (Millipore,AP124P; Darmstadt, Germany).

Determination of antioxidant enzymes

For the antioxidant enzyme assays, 0.3 g of each leaf sample was thoroughly ground with 3 mL of ice-cold 50 mM phosphate buffer (pH 7.8) containing 0.2 mM EDTA, 2 mM L-ascorbic acid, and 2% (w/v) polyvinylpolypyrrolidone. The homogenates were centrifuged at 12000 g for 20 min at 4°C. The resulting supernatants were used to determine the activities of APX, MDAR, DHAR and GR (Xia et al., 2009).

RNA extraction and gene expression analysis

Total RNA extractions were performed using an RNAprep pure Plant Kit (TIANGEN, Beijing, China) according to the instructions. The cDNA template for real time RT-PCR was synthesized using a Rever-Tra Ace qPCR RT Kit with a genomic DNA-removing enzyme (Toyobo, Osaka, Japan). qPCR was performed in a LightCycler480 detection system (Roche, Penzberg, Germany) using SYBR SuperMix

(Takara, Japan). The thermal cycling program ran at 95℃ for 3 min，followed by 40 cycles of 95℃ for 30 s ，57℃for 20 s，and 72℃ for 30 s. The primers for the target genes are shown in Supplemental Table S1. The tomato UBI3 and ACTIN2 genes were used as internal control. The relative gene expression was calculated using relative quantification $2^{-\Delta\Delta CT}$ method (Livak and Schmittgen., 2001) with normalization of data to the geometric mean of the internal control genes as recommended by Lovdal and Lillo (2009).

Yeast one-hybrid assays

Y1H assay was performed according to the instructions of the Matchmatch™ Gold Yeast One-Hybrid System (Clontech, USA). The 1937-bp promoter sequence of tomato RBOH1 were cloned into pAbAi to create the pAbAi-baits and the full-length BZR1 was sub cloned into pGADT7 to create the AD-prey vector,(primers are listed in Supplementary Table S2). pAbAi-baits were firstly linearized at BbsI site before them were transformed into Y1HGold and were screened on selective synthetic dextrose medium (SD) uracil. To confirm that the plasmids had integrated correctly into the genome of Y1HGold, Colony PCR analysis were performed using Matchmaker Insert Check PCR Mix 1(Clontech, USA). the Minimal Inhibitory Concentration of Aureobasidin A for the bait strains were determined before the AD-prey vectors were transformed into the bait strain. the transformants were screened on SD/-Leu/ AbA media. All transformations and screenings were repeated three times. Auto activation and transcription factor–protein interaction analysis were carried out according to the manufacturer's protocol.

Chromatin immunoprecipitation (Chip)

Chip was carried out using the EpiQuiK^{TM} Plant ChIP kit (Epigentek, Farmingdale, USA), as described in the manufacturer's protocol. Approximately 1g of leaf samples were collected from four-week-old 35Spro:BZR1-HA or wild-type seedlings grown under 4℃ for 12 hours. The DNA fragments combined with BZR1 protein were co-immunoprecipitated with an anti-HA antibody (Pierce; Rockford, USA). Goat anti-mouse IgG antibody (Millipore, Darmstadt, Germany) was used as the negative control. The enriched DNA fragments were quantified by qRT-PCR using the primers listed in Supplemental Table S3.

Statistical analysis

The experimental design was a completely randomized block design. An analysis of variance (ANOVA) was used to test for significance. When the interaction terms were significant ($P < 0.05$), the differences between the means were analyzed using Tukey comparisons. Significant differences between treatment means are indicated by different letters.

Accession Numbers

Sequence data of the genes investigated from this article can be found in Supplementary Table S1.

ACKNOWLEDGMENTS

We are grateful to the Tomato Genetics Resource Center at the California University, Davis, for supplying mutants. This work was supported by the State Key Program of National Natural Science Foundation of China (31430076).

Supplemental Data

The following supplemental materials are available.

Supplemental Table 1. Primer sequences used for qRT- PCR.

Supplemental Table 2. Primers used for pAbAi-baits and AD-prey constructs.

Supplemental Table 3. Primers used for ChIP-qPCR analysis.

Supplemental Figure 1. Role of DWARF in the relative electrolyte leakage after chilling stress.

Supplemental Figure 2. Role of DWARF in the induction of NPQ under control condition and the qE after chilling stress.

Supplemental Figure 3. Role of DWARF in the transcript of ORR, PGR5-LikeA1 and PGR5-Like A2.

Supplemental Figure 4. Role of BZR1 in the BR-regulated relative electrolyte leakage after chilling stress.

Supplemental Figure 5. Effects of BZR1 on the BR-regulated NPQ and qE.

Supplemental Figure 6. Effects of BZR1 on the BR-induced accumulation of H_2O_2.

Supplemental Figure 7. Silencing efficiency and the relative electrolyte leakage of RBOH1-RNAi plants in response to chilling stress.

Supplemental Figure 8. Role of RBOH1 in the BR-regulated NPQ and qE.

Supplemental Figure 9. PGR5 was involved in BR-induced chilling tolerance.

Supplemental Figure 10. Role of PGR5 in the BR-regulated NPQ under contol condition.

LITERATURE CITED

Akahashi S, Murata N (2005) Interruption of the Calvin cycle inhibits the repair of photosystem II from photodamage. Biochim. Biophys. Acta **1708**: 352-361

Allakhverdiev SI, Los DA, Mohanty P, Nishiyama Y, Murata N (2007) Glycinebetaine alleviates the inhibitory effect of moderate heat stress on the repair of photosystem II during photoinhibition. Biochim. Biophys. Acta **1767:** 1363-1371

Allakhverdiev, SI, Murata N (2004) Environmental stress inhibits the synthesis de-novo of proteins involved in the photodamage-repair cycle of Photosystem II in Synechocystis sp PCC 6803. Biochim. Biophys. Acta **1657:** 23-32

Asada K (2006) Production and scavenging of reactive oxygen species in chloroplasts and their functions. Plant Physiol **141:** 391-396

Bajguz A, Hayat S (2009) Effects of brassinosteroids on the plant responses to environmental stresses. Plant Physiol Bioch **47:** 1-8

Baker NR (2008) Chlorophyll fluorescence: A probe of photosynthesis in vivo. Annu. Rev. plant Biol **59:** 89-113

Casano LM, Martín M, Sabater B (2001) Hydrogen peroxide mediates the induction of chloroplastic Ndh complex under photooxidative stress in barley. Plant Physiol **125:**1450-1458

Clouse SD (2011) Brassinosteroid signal transduction: from receptor kinase activation to transcriptional networks regulating plant development. Plant Cell **23:**1219-1230

Danon A (2002) Redox reactions of regulatory proteins: do kinetics promote specificity? Trends Biochem. Sci **27:** 197-203

Deng XG, Zhu T, Zou LJ , Han XY, Zhou X, Xi DH, Zhang DW, Lin HH (2016) Orchestration of hydrogen peroxide and nitric oxide in brassinosteroid-mediated systemic virus resistance in Nicotiana benthamiana. Plant J 85: 478-493

Foyer CH, Souriau N, Perret S, Lelandais M, Kunert KJ, Pruvost C, Jouanin L (1995) Overexpression of glutathione reductase but not glutathione synthetase leads to increase in antioxidant capacity and resistance to photoinhibition in poplar trees. Plant Physiol **109:** 1047-1057

Garg N, Manchanda G (2009) ROS generation in plants: boon or bane? Plant Biosyst **143:** 81-96

Goss R, Lepetit B (2015) Biodiversity of NPQ. J. Plant Physiol **172:** 13-32

Guo ZX, Wang F, Xiang X, AhammedG J, Wang MM, Onac E, Zhou J, Xia XJ, Shi K, Yin XR, Chen KS, Yu JQ, et al (2016) Systemic induction of photosynthesis via illumination of the shoot apex is mediated sequentially by phytochrome B, auxin and hydrogen peroxide in tomato. Plant Physiol **172:**1-14

Han H, Gao S, Li B, Dong XC, Feng HL, Meng QW (2010) Overexpression of violaxanthin de-epoxidase gene alleviates photoinhibition of PSII and PSI in tomato during high light and chilling stress. J Plant Physiol **167:**176-183

Hashimoto M, Endo T, Peltier G, Tasaka M, Shikanai T (2003) A nucleus-encoded factor, CRR2, is essential for the expression of chloroplast ndhB in Arabidopsis. Plant J **36:** 541-549

Ikeuchi M, Uebayashi N, Sato F, Endo T (2014) Physiological functions of PsbS-dependent and PsbS-independent NPQ under naturally fluctuating light conditions. Plant Cell Physiol **55:**1286-1295

Jahns P, Holzwarth AR (2012) The role of the xanthophyll cycle and of lutein in photoprotection of photosystem II. Biochim. Biophys. Acta **1817:**182-193

Jakubowska D, Janicka M (2017) The role of brassinosteroids in the regulation of the plasma membrane H+-ATPase and NADPH oxidase under cadmium stress. Plant Science **264:**37-47

Johnson GN (2011) Reprint of: physiology of PSI cyclic electron transport in higher plants. Biochim. Biophys. Acta **1807:**906-911

Kromdijk J, Głowacka K, Leonelli L, Gabilly ST, Iwai M, Niyogi KK, Long SP (2016) Improving photosynthesis and crop productivity by accelerating recovery from photoprotection. Science **354:** 857-861

Lascano HR, Casano, LM, Martín M, Sabater B (2003) The activity of the chloroplastic Ndh complex is regulated by phosphorylation of the NDH-F subunit. Plant Physiol **132:** 256-26

Li H, Ye KY, Shi YT, Cheng JK, Zhang XY, Yang SH (2017) BZR1 positively regulates freezing tolerance via CBF-dependent and CBF independent pathways in Arabidopsis. Mol Plant **10:** 545-559

Li XJ, Chen XJ, Guo X, Yin LL, Ahammed GJ, Xu CJ, Chen KS, Liu CC, Xia XJ, Shi K, Zhou J, Zhou YH, et al (2016) DWARF overexpression induces alteration in phytohormone homeostasis, development, architecture and carotenoid accumulation in tomato. Plant Biotechnol J **14:** 1021-1033

Li XP, Bjorkman O, Shih C, Grossman AR, Rosenquist M, Jansson S, Niyogi KK (2000) A pigment-binding protein essential for regulation of photosynthetic light harvesting. Nature **403:** 391-395

Li XP, Muller-Moule P, Gilmore AM, Niyogi KK (2002) PsbS-dependent enhancement of feedback de-excitation protects photosystem II from photoinhibition. Proc Natl Acad Sci USA **99:** 15222–15227

Livak KJ, Schmittgen TD (2001) Analysis of relative gene expression data using real-time quantitative PCR and the $2^{-\Delta\Delta CT}$ method. Methods **25:**402–408

Lovdal T, Lillo C (2009) Reference gene selection for quantitative real-time PCR normalization in tomato subjected to nitrogen, cold, and light stress. Anal Biochem **387:** 238-242

Luo XT, Cai BD, Yu Lei, Ding J, Feng YQ (2018) Sensitive determination of brassinosteroids by solid phase boronate affinity labeling coupled with liquid chromatography-tandem mass spectrometry. J Chromatogr A **1546:**10-17

Lv XZ, Li, HZ,Chen XX, Xiang X, Guo ZX, Yu, JQ, Zhou, YH (2018) The role of calcium-dependent protein kinase in hydrogen peroxide, nitric oxide and ABA-dependent cold acclimation. J Exp Bot **69:** 127-4139

Maruta T, Tanouchi A, Tamoi M, Yabuta Y, Yoshimura K, Ishikawa T, Shigeoka S (2010) Arabidopsis chloroplastic ascorbate peroxidase isoenzymes play a dual role in photoprotection and gene regulation under photooxidative stress. Plant Cell

Physiol **51:** 190-200

Munekage Y, Hashimoto M, Miyake C, Tomizawa KI, Endo T, Tasaka M, Shikanai T (2004) Cyclic electron flow around photosystem I is essential for photosynthesis. Nature **429:** 579-582

Munekage Y, Hojo M, Meurer J, Endo T, Tasaka M, Shikanai T (2002) PGR5 is involved in cyclic electron flow around photosystem I and is essential for photoprotection in Arabidopsis. Cell **110:** 361-371

Murchie EH, Niyogi KK (2011) Manipulation of photoprotection to improve plant photosynthesis. Plant Physiol **155:** 86-92

Nishikawa Y, Yamamoto H, Okegawa Y, Wada S, Sato N, Taira Y, Sugimoto K. Makino A, Shikanai T (2012) PGR5-dependent cyclic electron transport around PSI contributes to the redox homeostasis in chloroplasts rather than CO_2 fixation and biomass production in rice. Plant Cell Physiol **53:**2117-2126

Nishiyama Y, Allakhverdiev SI, Murata N (2006) A new paradigm for the action of reactive oxygen species in the photoinhibition of photosystem II. Biochim. Biophys. Acta **1757:** 742-749

Niyogi KK, Grossman AR, Bjorkman O (1998) Arabidopsis mutants define a central role for the xanthophyll cycle in the regulation of photosynthetic energy conversion. Plant Cell **10:** 1121-1134

Ogweno JO, Song XS, Shi K, Hu WH, Mao WH, Zhou YH, Yu JQ, Nogues S (2008) Brassinosteroids alleviate heat-induced inhibition of photosynthesis by increasing carboxylation efficiency and enhancing antioxidant systems in Lycopersicon esculentum Plant Growth Regul **27**:49-57

Oh MH, Sun J, Oh DH., Zielinski RE, Clouse SD Huber SC (2011) Enhancing Arabidopsis leaf growth by engineering the BRASSINOSTEROID INSENSITIVE1 receptor kinase. Plant Physiol **157:** 120-131

Oxborough K, Baker NR (1997) Resolving chlorophyll a fluorescence images of photosynthetic efficiency into photochemical and non-photochemical components-calculation of qP and Fv'/Fm' without measuring Fo. Photosynth Res **54:**135-142

Pinnola A, Dall'Osto L, Gerotto C, Morosinotto T, Bassi R, Alboresi A (2013)

Zeaxanthin binds to light-harvesting complex stress-related protein to enhance nonphotochemical quenching in Physcomitrella patens. Plant Cell **25:**3519-3534

She J, Han Z, Kim TW, Wang J, Cheng W, Chang J, Shi S, Wang J, Yang M, Wang ZY, Chai JJ (2011) Structural insight into brassinosteroids perception by BRI1. Nature **474:** 472-476

Shikanai T(2007) Cyclic electron transport around photosystem I: Genetic approaches. Annu Rev plant Biol **58:** 199-217

Small CC, Degenhardt D (2018) Plant growth regulators for enhancing revegetation success in reclamation: A review. Ecol Eng **118:** 43–51

Steinbeck J, Nikolova D, Weingarten R, Johnson X, Richaud P, Peltier G, Hermann M, Magneschi L, Hippler M (2015) Deletion of Proton Gradient Regulation 5 (PGR5) and PGR5-Like 1 (PGRL1) proteins promote sustainable light-driven hydrogen production in Chlamydomonas reinhardtii due to increased PSII activity under sulfur deprivation. Front Plant Sci **6:** 892

Strand DD, Livingston AK, Satoh CM, Froehlich JE, Maurino VG, Kramer DM (2015) Activation of cyclic electron flow by hydrogen peroxide in vivo. Proc Natl Acad Sci USA **112**: 5539-5544

Sun Y, Fan XY, Cao DM, Tang W, He K, Zhu JY, He JX, Bai MY, Zhu S, Oh E, Patil S, Kim TW, et al (2010) Integration of brassinosteroid signal transduction with the transcription network for plant growth regulation in Arabidopsis. Dev Cell **19:** 765-777

Takahashi S, Badger MR (2011) Photoprotection in plants: a new light on photosystem II damage. Trends Plant Sci **16:** 53-60

Takahashi S, Milward, SE, Fan DY, Chow WS. and Badger MR (2009) How does cyclic electron flow alleviate photoinhibition in Arabidopsis? Plant Physiol **149**:1560-1567

Takahashi S, Murata N (2008) How do environmental stresses accelerate photoinhibition? Trends Plant Sci **13:** 178-182

Tarkowska D, Novak O, Oklestkova J, Strnad M (2016) The determination of 22 natural brassinosteroids in a minute sample of plant tissue by UHPLC-ESI-MS/MS.

Anal Bioanal Chem **408:** 6799-6812

Triantaphylides C, Havaux V (2009) Singlet oxygen in plants: production, detoxification and signaling. Trends Plant Sci **14:** 219-228

Wang F, Guo ZX, Li HZ, Wang MM, Onac E, Zhou J, Xia XJ, Shi K, Yu JQ, Zhou YH (2016) Phytochrome A and B function antagonistically to regulate cold tolerance via abscisic acid-dependent jasmonate signaling. Plant Physiol **170:** 459-471

Wang F, Wu N, Zhang LY, Ahammed GJ, Chen XX, Xiang X, Zhou J, Xia XJ, Shi K, Yu JQ, Foyer CH, Zhou YH (2018a) Light signaling-dependent regulation of photoinhibition and photoprotection in tomato. Plant Physiol **176:**1311-1326

Wang Y, Cao JJ, Wang KX, Xia XJ, Shi K, Zhou YH, Yu JQ, Zhou J (2018b) BZR1 mediates brassinosteroid-induced autophagy and nitrogen starvation in tomato. Plant Physiol **DOI:**10.1104/pp.18.01028

Wang ZY, Nakano T, Gendron J, He JX, Chen M, Vafeados D, Yang YL, Fujioka S, Yoshida S, Asami T, Chory J (2002) Nuclear-localized BZR1 mediates brassinosteroid-induced growth and feedback suppression of brassinosteroid biosynthesis. Dev. Cell, **2:** 505–513

Xia XJ, Fang PP, Guo X, Qian XJ, Zhou J, Shi K, Zhou YH, Yu JQ (2017) Brassinosteroid-mediated apoplastic H_2O_2-glutaredoxin 12/14 cascade regulates antioxidant capacity in response to chilling in tomato. Plant Cell Environ **41:**1052-1064

Xia XJ, Wang YJ, Zhou YH, Tao Y, Mao WH, Shi K, Asami T, Chen ZX, Yu JQ(2009) Reactive oxygen species are involved in brassinosteroid-induced stress tolerance in cucumber. Plant Physiol **150:** 801-814

Xia XJ, Zhou YH, Shi K, Zhou J, Foyer CH ,Yu, JQ (2015) Interplay between reactive oxygen species and hormones in the control of plant development and stress tolerance. J Exp Bot **66:** 2839-2856

Yin YL, Qin KZ, Song XW, Zhang QH, Zhou YH, Xia XJ, Yu, JQ (2018) BZR1 transcription factor regulates heat stress tolerance through FERONIA receptor-like kinase-mediated reactive oxygen species signaling in tomato. Plant Cell Physiol **59:** 2239–2254

Zhou J, Wang J, Li X, Xia XJ, Zhou YH, Shi K, Chen ZX, Yu JQ(2014) H_2O_2 mediates the crosstalk of brassinosteroid and abscisic acid in tomato responses to heat and oxidative stresses. J Exp Bot **65:** 4371-4383

Zurbriggen MD, Carrillo N, Hajirezaei MR (2010) ROS signaling in the hypersensitive response: when, where and what for? Plant Signal Behav 5: 393-39

Figure legends

Figure 1. Regulation of photoprotection by BR in tomato plants. A, Maximum quantum efficiency of photosystem II (Fv/Fm) and maximum amount of photooxidizable P700 (ΔP700max) in the dwf mutant, wild type (WT) and transgenic line overexpressing DWARF (DWF:OE) after exposure to 4℃ for 6 d. B, Kinetics of NPQ induction following exposure to light for 5 min in plants at 3 d during chilling. C and D, The postillumination chlorophyll fluorescence (CEF around PSI，C) at 3 d and the relative expression level of PGR5 (D) at 6 h after the exposure of plants to 4℃. E, Accumulation of the PsbS, VDE and D1 proteins in plants after expourue to 4℃ for 24 h. The data represent the means of 4 biological replicates (±SD). Different letters indicate significant differences ($P < 0.05$) according to the Tukey's test.

Figure 2. Chilling increased the accumulation of brassinosteroids and BZR1 proteins. A, Brassinosteroids contents in tomato leaves exposed to 25℃ and 4℃ for 6, 12 and 24 hours. B, Brassinosteroids contents in the dwf mutant, wild type (WT) and transgenic line overexpressing DWARF (DWF:OE) after exposure to 4℃ for 6 h. C, Accumulation of BZR1 protein at 25℃ and 4℃ as influenced by the application of 24-epibrassinolide (EBR, 0.2μM). Samples were collected at 12 h after chilling. Transgenic line with HA tag (35Spro:BZR1-HA) were used for analysis for BZR1 protein. The data represent the means of 4 biological replicates (±SD). Asterisks indicate significant differences according to the Student's t-test at 0.05% level. Different letters indicate significant differences ($P < 0.05$) according to Tukey's test. BL, brassinolide; CS, castasterone; 28-norCS, 28-norcastasterone.

Figure 3. Regulation of photoprotection by BZR1 in tomato plants. A, Fv/Fm and ΔP700max in plants after exposure to 4℃ for 6 d. B, Kinetics of NPQ induction following exposure to light for 5 min in plants at 3 d during chilling. C and D, The postillumination chlorophyll fluorescence (CEF around PSI, C) at 3 d and transcript levels of PGR5 (D) at 6 h after the exposure of plants to 4℃. E, Accumulation of PsbS, VDE and D1 proteins in plants after exposure to 4℃ for 24 h. Twenty-four hours before chilling, the plants were treated with 0.2 μM 24-epibrassinolide (EBR) or distilled water as control. The data represent means of 4 biological replicates (±SD). Different letters indicate significant differences ($P < 0.05$) according to Tukey's test.

Figure 4. Activation of RBOH1 transcript and H_2O_2 production by BZR1. A , The transcript levels of RBOH1. B, Cytochemical detection of H_2O_2. Black arrows indicate H_2O_2 in the apoplast. Leaf Samples were harvested from the plants at 6 h after chilling at 4℃. C, BRRE and E-boxes in the tomato RBOH1 promoter sequence. Numbering is from predicted transcriptional start sites. D, Yeast-one hybrid analysis of BZR1 binding to the the RBOH1 promoter in tomato. The 1937-bp promoter sequence of RBOH1 indicated in (C) was cloned into the pAbAi vector to construct pAbAi-bait. Interaction was determined on SD medium lacking leucine in the presence of AbA (–Leu+AbA^{100}). E, Chip-qPCR analysis of BZR1 binding to the RBOH1 promoter in tomato. Transgenic line with HA tag (35Spro:BZR1-HA) at 6-leaf stage were exposed to 4℃ and input chromatin was isolated from leaf samples at 12 h. The epitope-tagged BZR1-chromatin complex was immunoprecipitated with an anti-HA anti- body. A control reaction was performed side-by-side using mouse IgG. Input- and ChIP-DNA samples were quantified by qRT-PCR. The ChIP results are presented as a percentage of the input DNA. The data represent the means of 4 biological replicates (±SD). Different letters indicate significant differences ($P < 0.05$) according to Tukey's test.

Figure 5. RBOH1 is involved in BR-regulated photoprotection in tomato plants. A, Fv/Fm and ΔP700max in plants after exposure to 4℃ for 6 d. B, Kinetics of NPQ induction following exposure to light for 5 min in plants at 3 d during chilling. C and

D, The postillumination chlorophyll fluorescence (CEF around PSI, C) at 3 d and transcript levels of PGR5 (D) at 6 h after the exposure of plants to 4℃. E, Accumulation of PsbS, VDE and D1 proteins in plants after exposure to 4℃ for 24 h. Twenty-four hours before chilling, the plants were treated with 0.2 μM 24-epibrassinolide (EBR) or distilled water as control. The data represent means of 4 biological replicates (±SD). Different letters indicate significant differences ($P < 0.05$) according to Tukey's test.

Figure 6. PGR5 is involved in BR-regulated photoprotection in tomato plants. A, Fv/Fm and ΔP700max in the wild type (WT) and pgr5 mutant plants after exposure to 4℃ for 6 d. B, Kinetics of NPQ induction following light exposure for 5 min and quantification of qE in plants at 3 d during chilling. C, Postillumination chlorophyll fluorescence (CEF around PSI) in plants at 3 d during chilling. D, Accumulation of the PsbS, VDE and D1 proteins in plants after exposure to 4℃ for 24 h. Twenty-four hours before chilling, the plants were treated with 0.2 μM 24-epibrassinolide (EBR) or distilled water as the control. The data represent the means of 4 biological replicates (±SD). Different letters indicate significant differences ($P < 0.05$) according to Tukey's test.

Figure 7. PGR5 is involved in the BR-induced ROS scavenging capacity of tomato plants. Samples were taken at 24 h after the chilling treatment. Twenty-four hours before chilling, the plants were treated with 0.2 μM 24-epibrassinolide (EBR) or distilled water as control. The data represent means of 4 biological replicates (±SD). Different letters indicate significant differences ($P < 0.05$) according to Tukey's test.

Figure 8. A proposed model for the regulation of photoprotection by brassinosteroids (BRs) in response to chilling stress. Chilling induced the accunmulation of BRs in plant. Induction by cold and BR, BZR1 directly activates the transcript of RBOH1 and the generation of apoplastic H_2O_2, subsequently induced the PGR5-dependent CEF, NPQ, and accumulation or activity of proteins involved in photoprotection.

Figure. 1

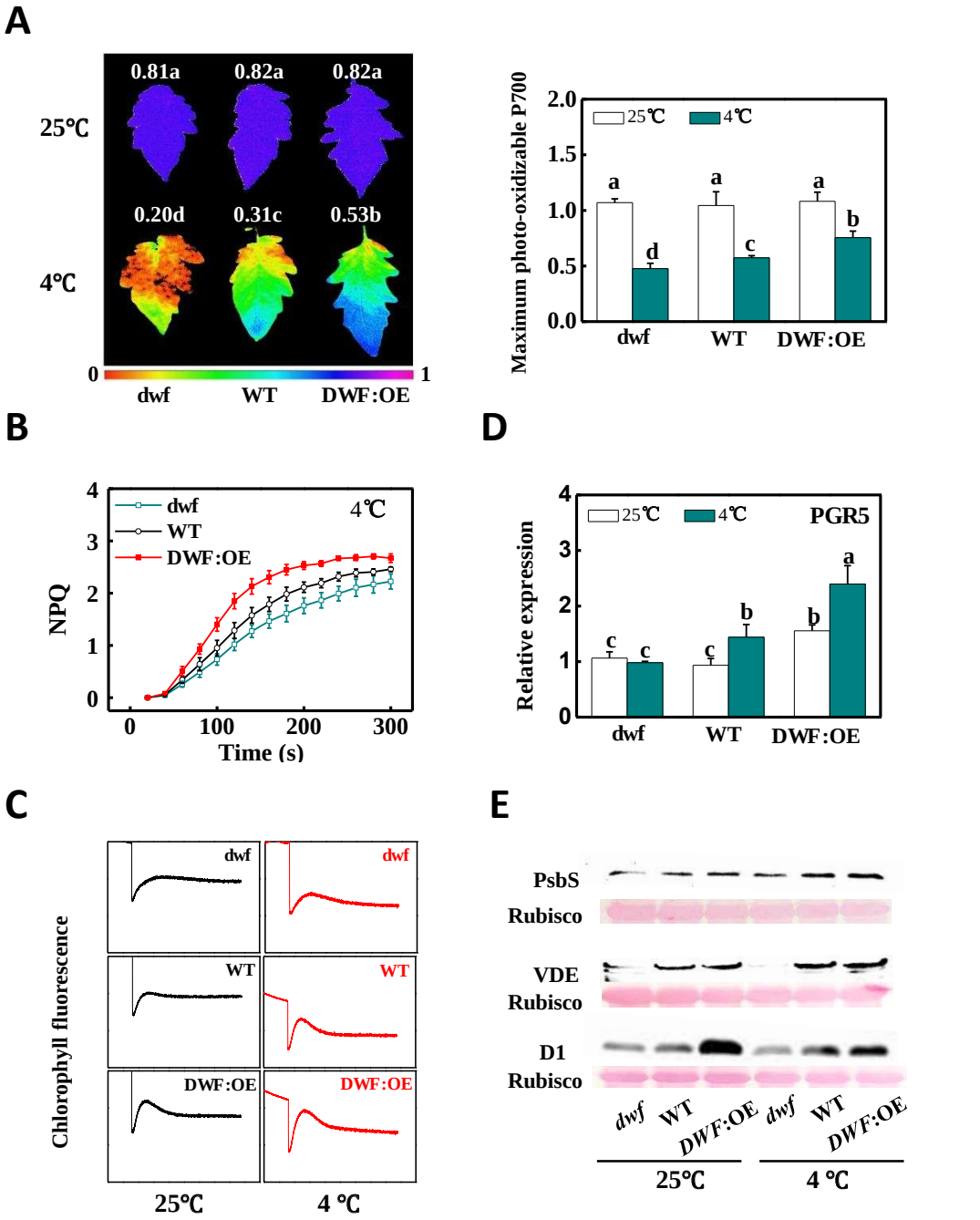
A
0.81a
0.82a
0.82a
25℃
0.20d
0.31c
0.53b
4℃
0
1
dwf
WT
DWF:OE
Maximum photo-oxidizable P700
25℃
4℃
a
d
a
c
a
b
dwf
WT
DWF:OE
B
NPQ
dwf
WT
DWF:OE
4℃
Time (s)
D
Relative expression
25℃
4℃
PGR5
dwf
WT
DWF:OE
C
Chlorophyll fluorescence
dwf
WT
DWF:OE
25℃
4 ℃
E
PsbS
Rubisco
VDE
Rubisco
D1
Rubisco
dwf
WT
DWF:OE
25℃
4 ℃

Figure. 2

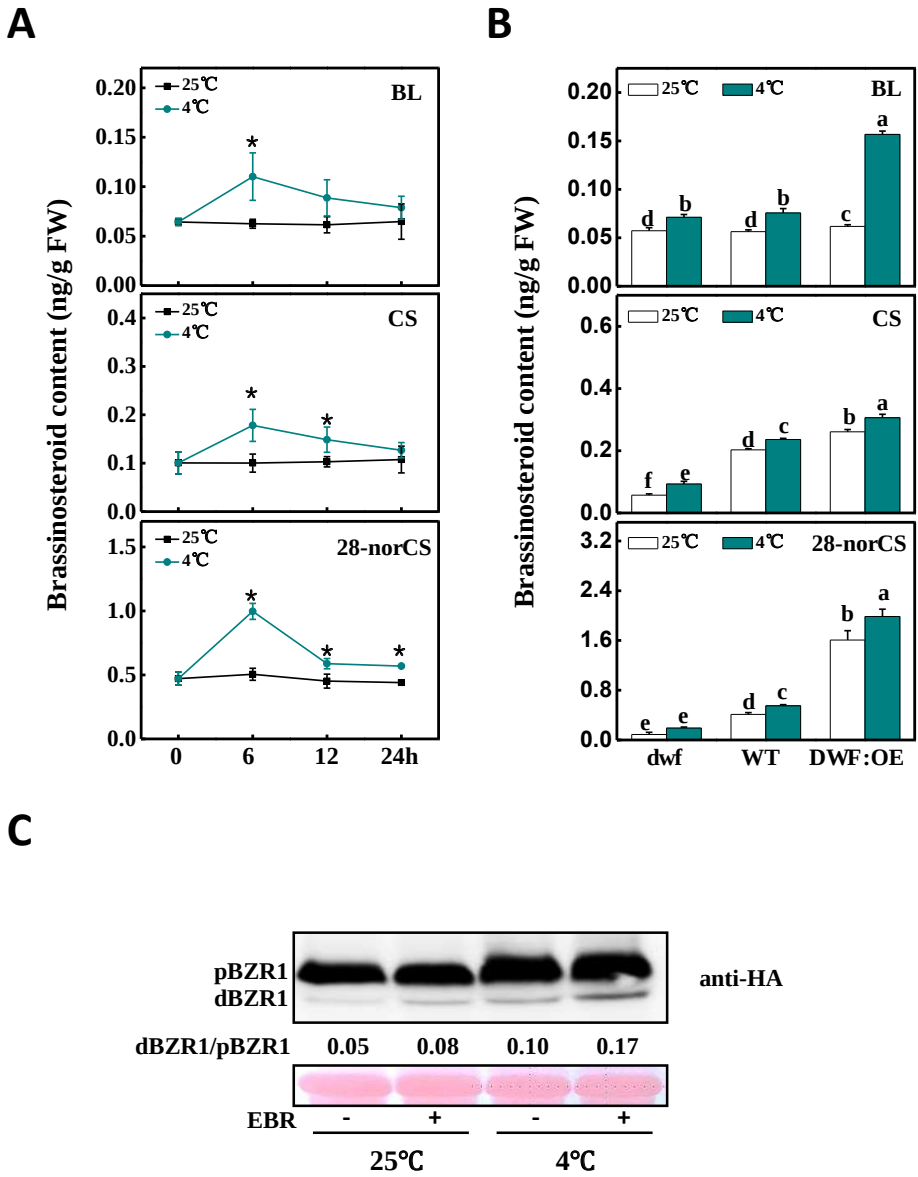
A
B
C
Brassinosteroid content (ng/g FW)
25℃
4℃
BL
CS
28-norCS
0
6
12
24h
dwf
WT
DWF:OE
pBZR1
dBZR1
anti-HA
dBZR1/pBZR1
0.05
0.08
0.10
0.17
EBR
25℃
4℃

Figure. 3

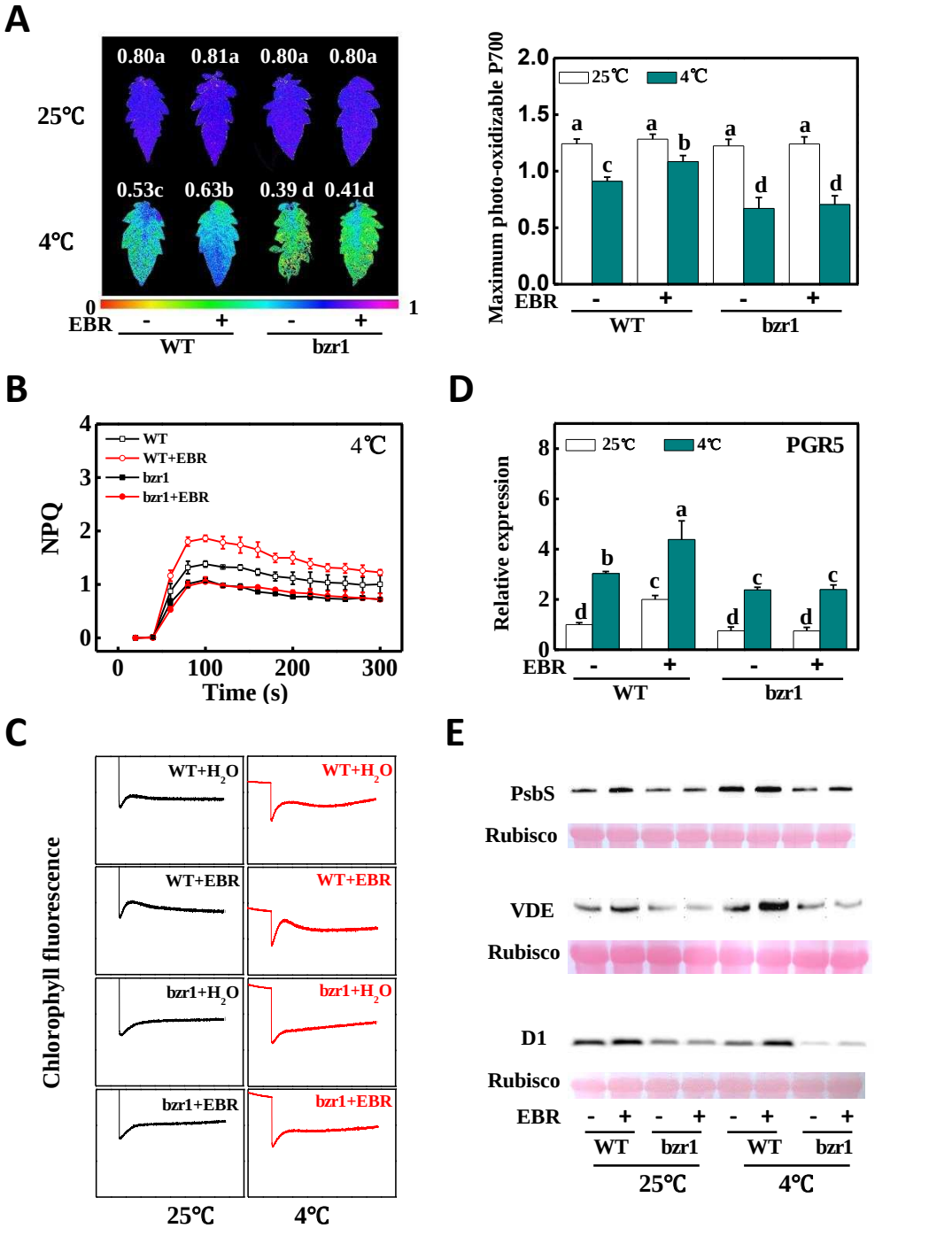
A
0.80a
0.81a
0.80a
0.80a
25℃
0.53c
0.63b
0.39 d
0.41d
4℃
0
1
EBR - + - +
WT
bzr1
Maximum photo-oxidizable P700
25℃
4℃
EBR - + - +
WT
bzr1
B
NPQ
4℃
WT
WT+EBR
bzr1
bzr1+EBR
Time (s)
D
Relative expression
25℃
4℃
PGR5
EBR - + - +
WT
bzr1
C
Chlorophyll fluorescence
WT+H2O
WT+EBR
bzr1+H2O
bzr1+EBR
25℃
4℃
E
PsbS
Rubisco
VDE
Rubisco
D1
Rubisco
EBR - + - + - + - +
WT
bzr1
WT
bzr1
25℃
4℃

Figure. 4

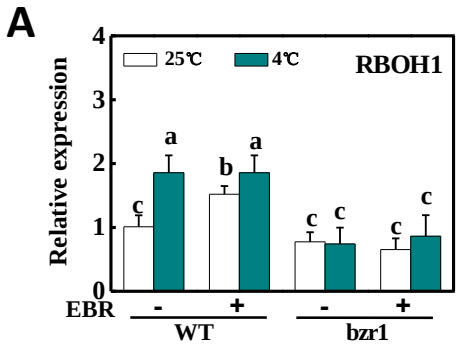
A
25℃
4℃
RBOH1
Relative expression
EBR
WT
bzr1

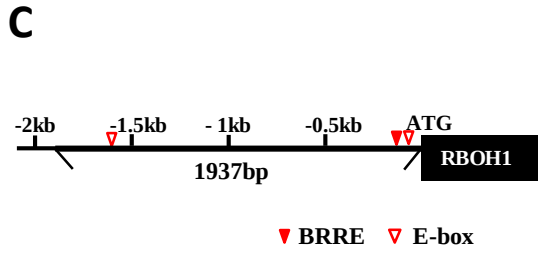
C
-2kb
-1.5kb
- 1kb
-0.5kb
ATG
1937bp
RBOH1
BRRE
E-box

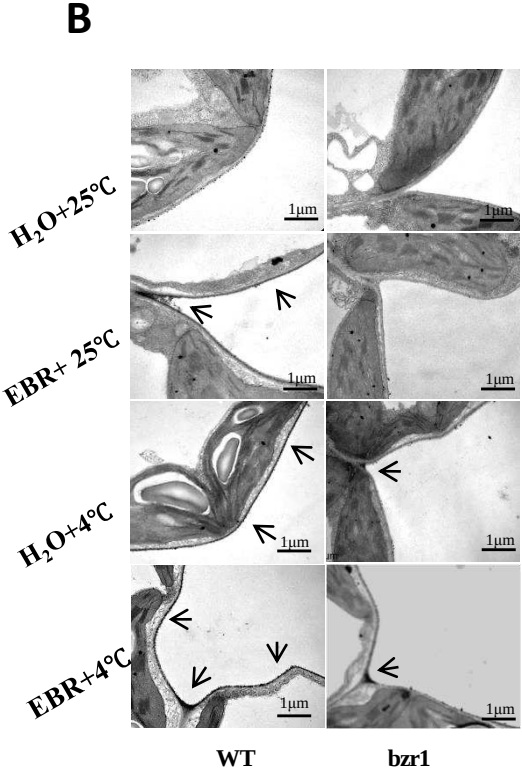
B
H2O+25℃
EBR+ 25℃
H2O+4℃
EBR+4℃
1μm
WT
bzr1

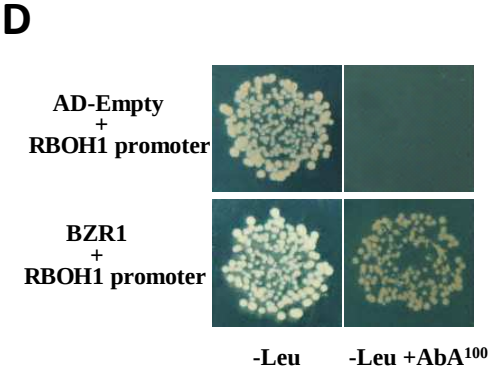
D
AD-Empty
+
RBOH1 promoter
BZR1
+
RBOH1 promoter
-Leu
-Leu +AbA100

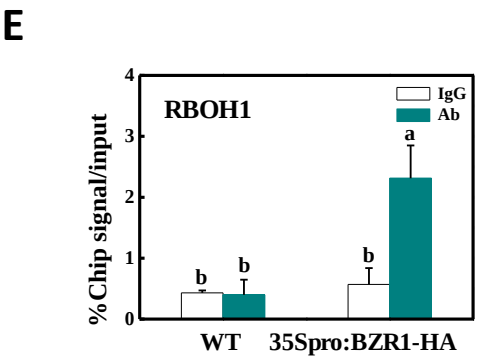
E
RBOH1
IgG
Ab
%Chip signal/input
WT
35Spro:BZR1-HA

Figure. 5

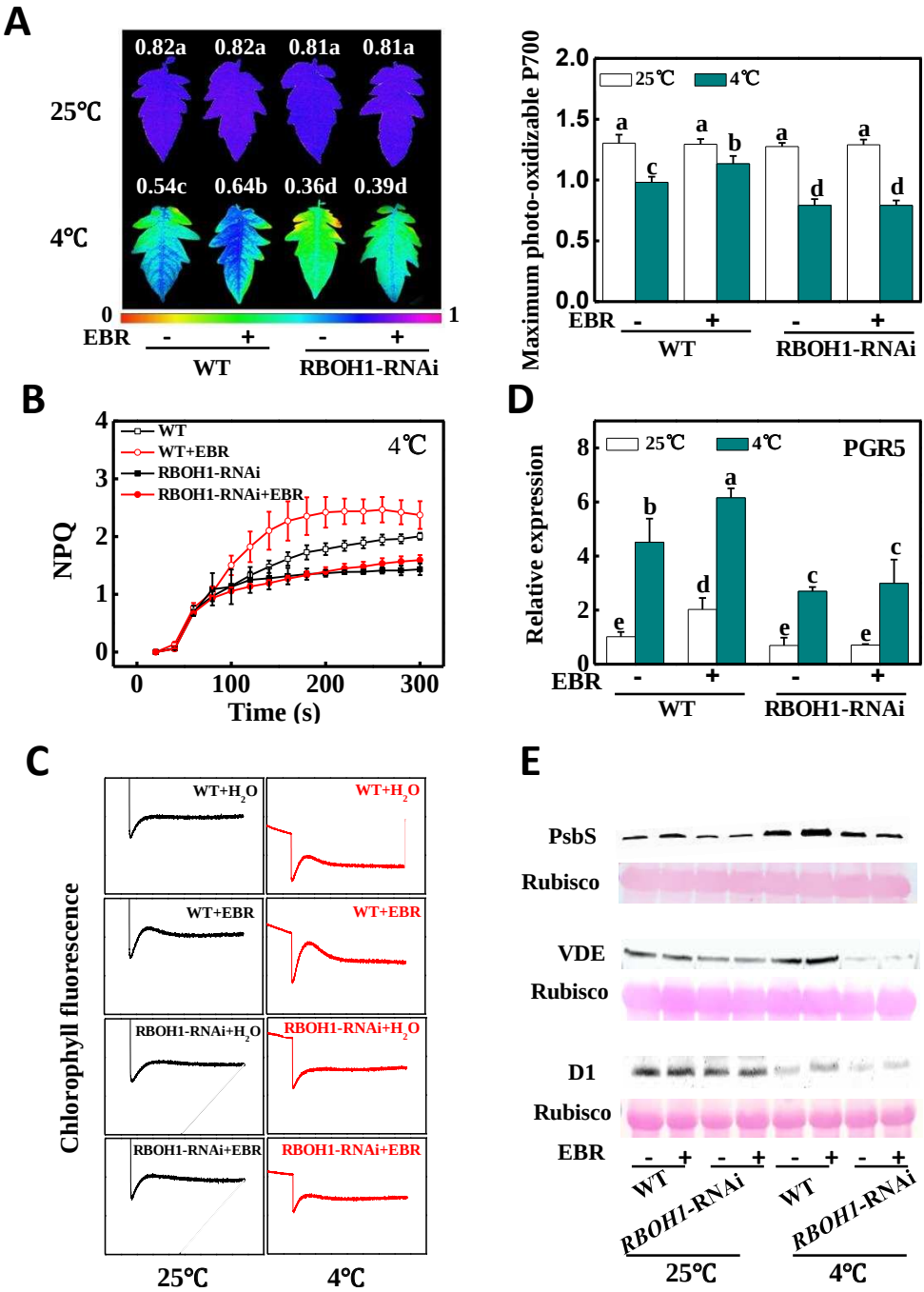
A
0.82a
0.82a
0.81a
0.81a
25℃
0.54c
0.64b
0.36d
0.39d
4℃
0
1
EBR
-
+
-
+
WT
RBOH1-RNAi
Maximum photo-oxidizable P700
25℃
4℃
2.0
1.5
1.0
0.5
0.0
a
c
a
b
a
d
a
d
EBR
-
+
-
+
WT
RBOH1-RNAi
B
NPQ
WT
WT+EBR
RBOH1-RNAi
RBOH1-RNAi+EBR
4℃
4
3
2
1
0
0
100
200
300
Time (s)
D
Relative expression
25℃
4℃
PGR5
8
6
4
2
0
e
b
d
a
e
c
e
c
EBR
-
+
-
+
WT
RBOH1-RNAi
C
Chlorophyll fluorescence
WT+H2O
WT+H2O
WT+EBR
WT+EBR
RBOH1-RNAi+H2O
RBOH1-RNAi+H2O
RBOH1-RNAi+EBR
RBOH1-RNAi+EBR
25℃
4℃
E
PsbS
Rubisco
VDE
Rubisco
D1
Rubisco
EBR
- + - + - + - +
WT
RBOH1-RNAi
WT
RBOH1-RNAi
25℃
4℃

Figure. 6

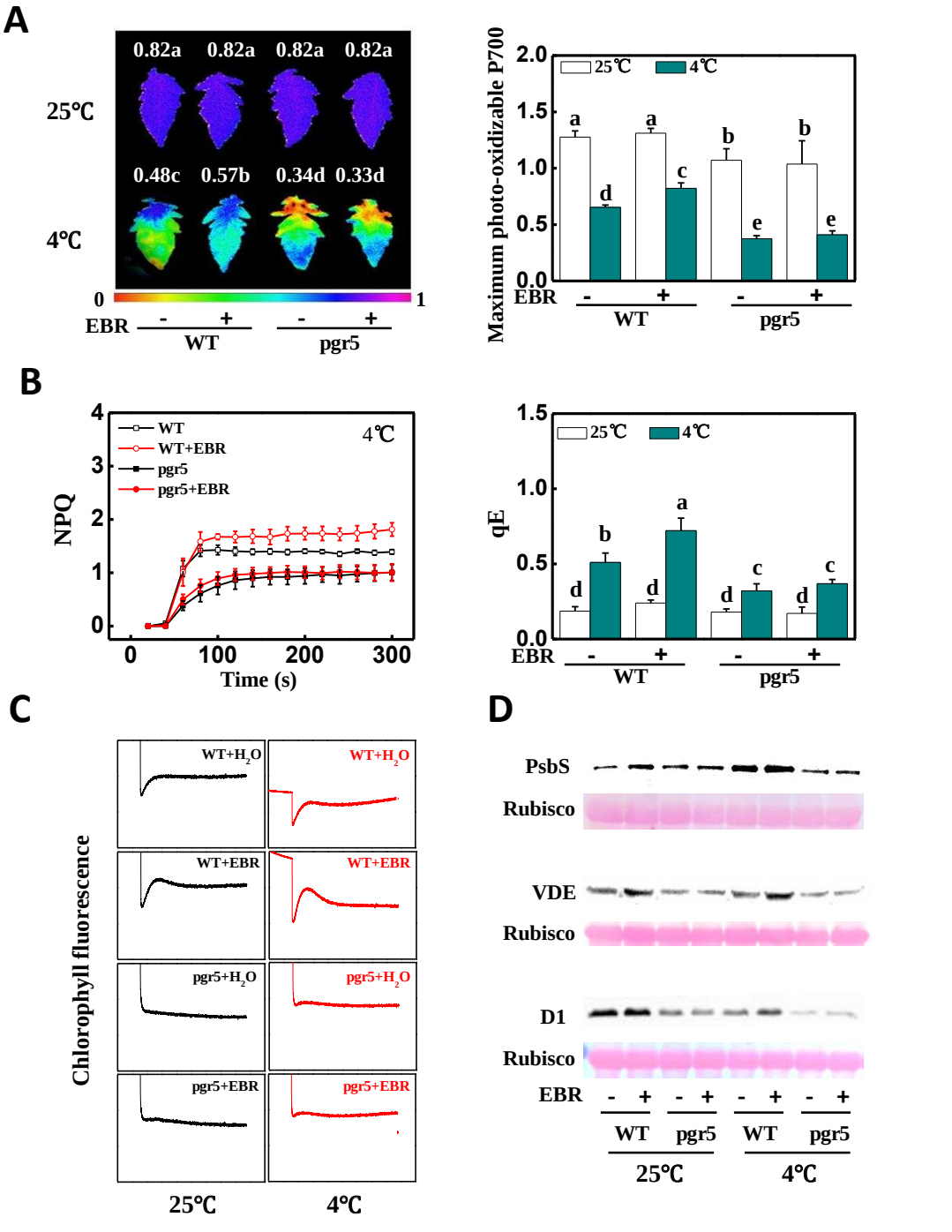
A
0.82a 0.82a 0.82a 0.82a
0.48c 0.57b 0.34d 0.33d
25℃
4℃
0
1
EBR - + - +
WT
pgr5
Maximum photo-oxidizable P700
25℃ 4℃
2.0
1.5
1.0
0.5
0.0
a a b b
d c e e
EBR - + - +
WT
pgr5
B
NPQ
WT
WT+EBR
pgr5
pgr5+EBR
4℃
Time (s)
qE
25℃ 4℃
d b a d c d c
C
Chlorophyll fluorescence
WT+H2O
WT+EBR
pgr5+H2O
pgr5+EBR
25℃
4℃
D
PsbS
Rubisco
VDE
Rubisco
D1
Rubisco
EBR - + - + - + - +
WT pgr5 WT pgr5
25℃ 4℃

Figure. 7

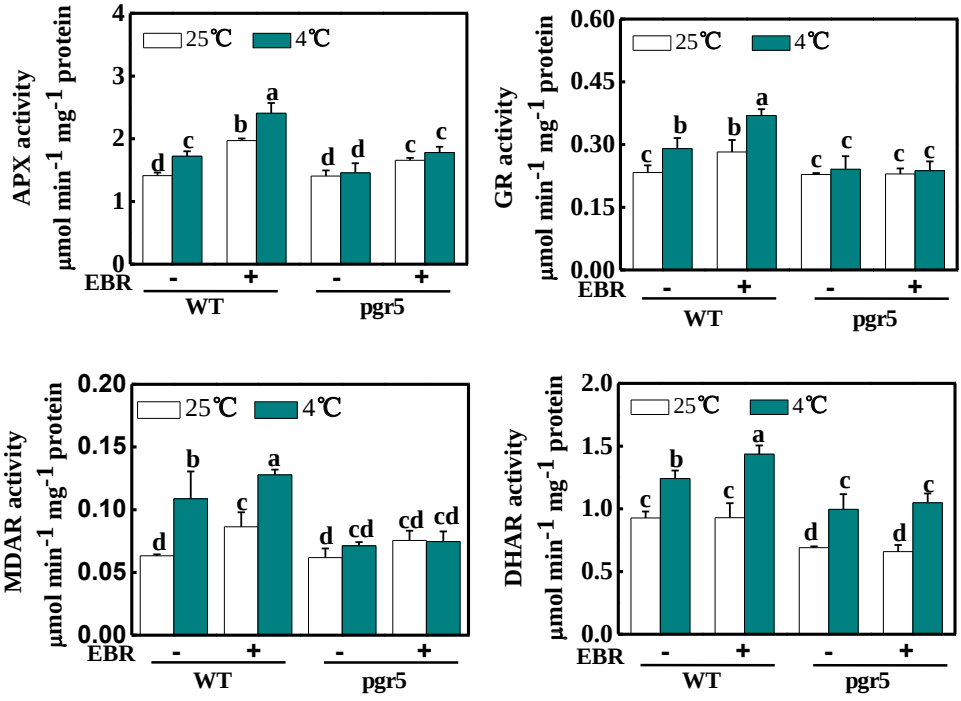
APX activity
μmol min-1 mg-1 protein
25℃
4℃
EBR
WT
pgr5
GR activity
μmol min-1 mg-1 protein
MDAR activity
μmol min-1 mg-1 protein
DHAR activity
μmol min-1 mg-1 protein

Figure. 8

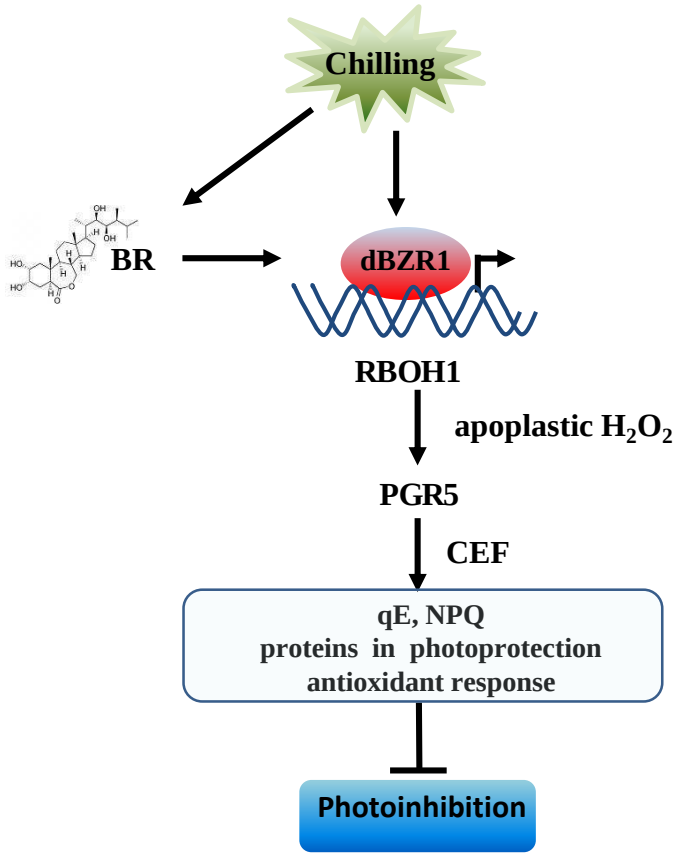
Chilling
BR
dBZR1
RBOH1
apoplastic H_2O_2
PGR5
CEF
qE, NPQ
proteins in photoprotection
antioxidant response
Photoinhibition

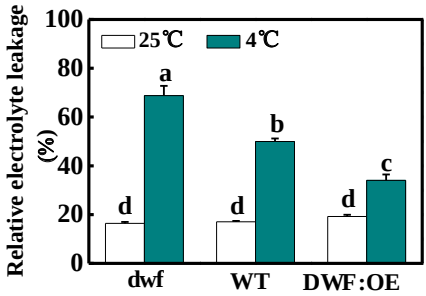

Supplemental Figure S1. Role of *DWARF* in the relative electrolyte leakage after chilling stress. Leaf samples from *dwf* mutants, wild type (WT) and transgenic lines overexpressing *DWARF* (*DWF*:OE) were collected at 6 d after chilling. The data represent the means of 4 biological replicates (±SD). Different letters indicate significant differences ($P < 0.05$) according to Tukey's test.

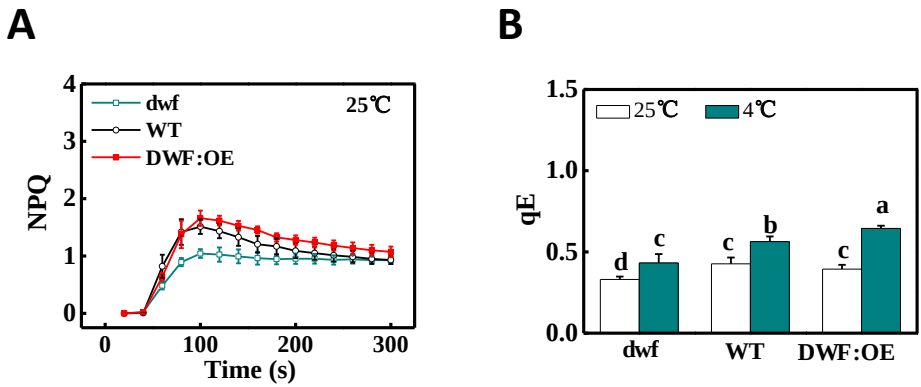

Supplemental Figure S2. Role of *DWARF* in the induction of NPQ under control condition and the qE after chilling stress. A and B, Kinetics of NPQ induction following exposure to light for 5 min (A) under control condition and the qE (B) under control and chilling conditions in *dwf* mutants, wild type (WT) and transgenic lines overexpressing *DWARF* (*DWF*:OE) plants. Measurements were performed at 3 d during chilling. The data represent the means of 4 biological replicates (±SD). Different letters indicate significant differences ($P < 0.05$) according to Tukey's test.

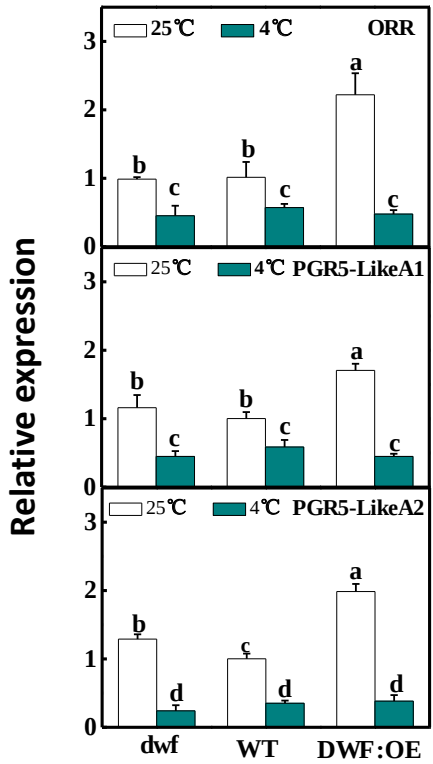

Supplemental Figure S3. Role of *DWARF* in the transcript of *ORR, PGR5-LikeA1 and PGR5-Like A2*. Leaf Samples from *dwf* mutants, wild type (WT) and transgenic lines overexpressing *DWARF* (*DWF*:OE) were collected at 6 h after chilling. The data represent the means of 4 biological replicates (±SD). Different letters indicate significant differences ($P < 0.05$) according to Tukey's test.

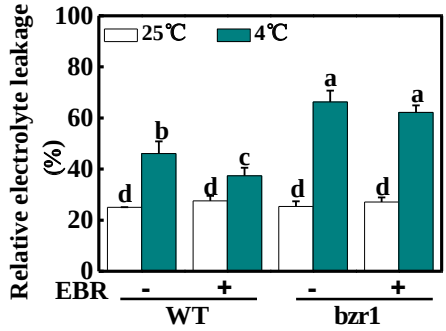

Supplemental Figure S4. Role of *BZR1* in the BR-regulated relative electrolyte leakage after chilling stress. Samples were collected at 6 d after chilling stress. Twenty-four hours before chilling, the plants were treated with 0.2 μM 24-epibrassinolide (EBR) or distilled water as the control. The data represent the means of 4 biological replicates (±SD). Different letters indicate significant differences ($P < 0.05$) according to Tukey's test.

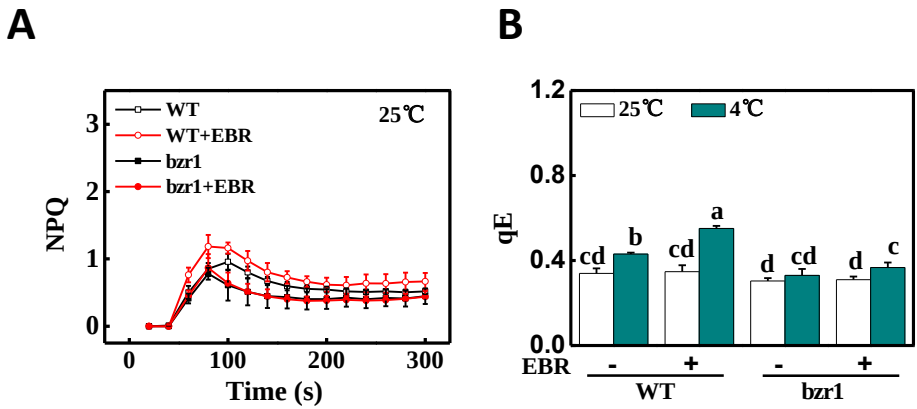

Supplemental Figure S5. Effects of *BZR1* on the BR-regulated NPQ and qE. A and B, Kinetics of NPQ induction following exposure to light for 5 min (A) under control condition and the qE (B) under control and chilling conditions in wild type (WT) and *bzr1* mutants. Measurements were performed at 3 d during chilling stress. Twenty-four hours before chilling, the plants were treated with 0.2 μM 24-epibrassinolide (EBR) or distilled water as the control. The data represent the means of 4 biological replicates (±SD). Different letters indicate significant differences ($P < 0.05$) according to Tukey's test.

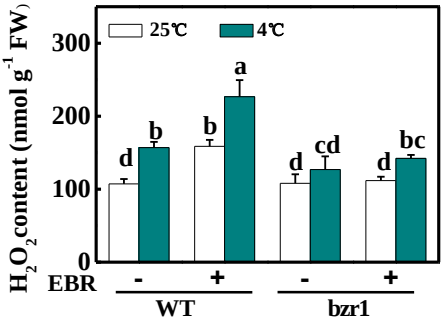

Supplemental Figure S6. Effects of *BZR1* on the BR-induced accumulation of H_2O_2. Tomato leaves from *bzr1* mutants and wild type plants (WT) were collected at 6 h after chilling. Twenty-four hours before chilling, the plants were treated with 0.2 μM 24- epibrassinolide (EBR) or distilled water as the control. The data represent the means of 4 biological replicates (±SD). Different letters indicate significant differences ($P < 0.05$) according to Tukey's test.

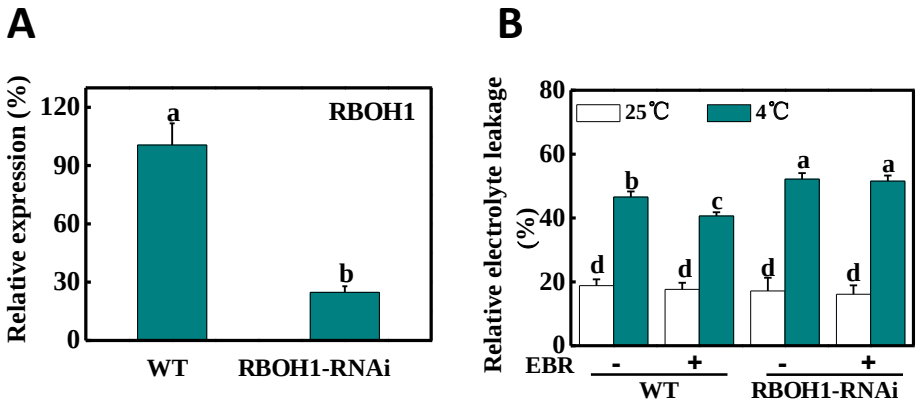

Supplemental Figure S7. Silencing efficiency and the relative electrolyte leakage of *RBOH1*-RNAi plants in response to chilling stress. A, Relative expression of *RBOH1* in the *RBOH1*-RNAi plants. Relative gene expression for *RBOH1* gene was calculated using the wild type (WT) plants as 1. B, Relative electrolyte leakage in WT and *RBOH1*-RNAi plants after exposed to chilling for 6 d. Twenty-four hours before chilling, the plants were treated with 0.2 μM 24-epibrassinolide (EBR) or distilled water as the control. The data represent the means of 4 biological replicates (±SD). Different letters indicate significant differences ($P < 0.05$) according to Tukey's test.

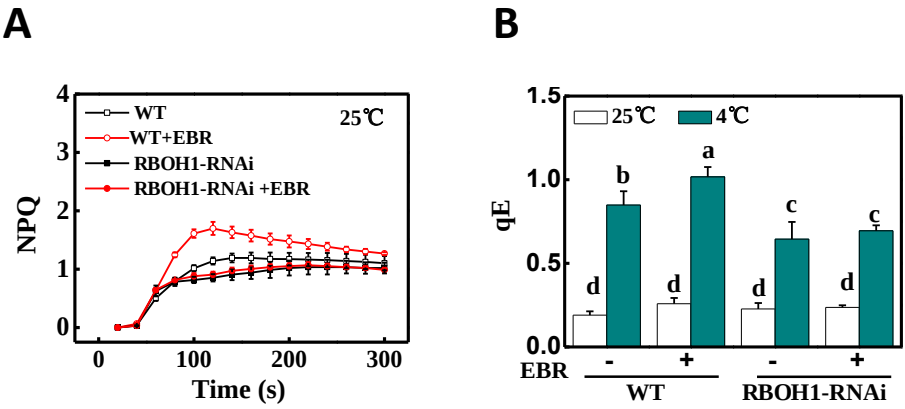

Supplemental Figure S8. Role of *RBOH1* in the BR-regulated NPQ and qE. A and B, Kinetics of NPQ induction following exposure to light for 5 min (A)under control condition and the qE (B) under control and chilling conditions in wild type (WT) and *RBOH1*-RNAi plants. Measurements were performed at 3d during chilling. Twenty-four hours before chilling, the plants were treated with 0.2 μM 24-epibrassinolide (EBR) or distilled water as the control. The data represent the means of 4 biological replicates (±SD). Different letters indicate significant differences ($P < 0.05$) according to Tukey's test.

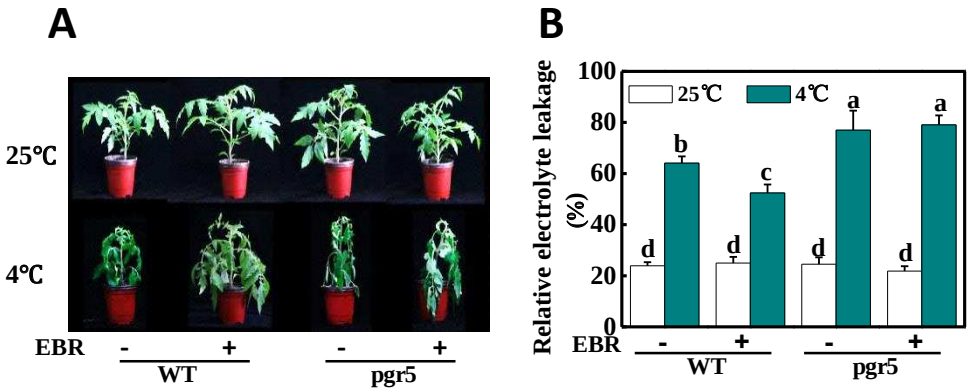

Supplemental Figure S9. *PGR5* was involved in BR-induced chilling tolerance. A and B, The phenotypes (A) and relative electrolyte leakage (B) of the wild type (WT) and *pgr5* mutant (*pgr5*) after exposure to chilling for 6 d. Twenty-four hours before chilling, the plants were treated with 0.2 μM 24-epibrassinolide (EBR) or distilled water as the control. The data represent the means of 4 biological replicates (±SD). Different letters indicate significant differences ($P < 0.05$) according to Tukey's test.

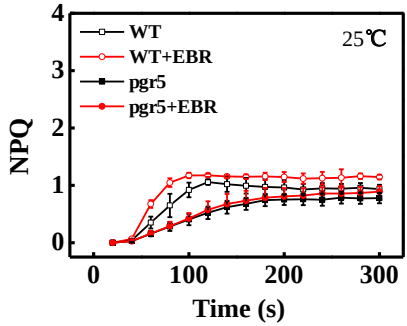

Supplemental Figure S10. Role of *PGR5* in the BR-regulated NPQ under control condition. Kinetics of NPQ induction following exposure to light for 5 min under control condition in the wild type (WT) and *pgr5* mutants (*pgr5*). Twenty-four hours before chilling, the plants were treated with 0.2 μM 24-epibrassinolide (EBR) or distilled water as the control. The data represent the means of 4 biological replicates (±SD). Different letters indicate significant differences ($P < 0.05$) according to Tukey's test.